DISSERTATION

CONSTRAINED DYNAMICS OF ROLLING BALLS AND MOVING ATOMS

Submitted by

Byungsoo Kim

Department of Mathematics

In partial fulfillment of the requirements

for the degree of Doctor of Philosophy

Colorado State University

Fort Collins, Colorado

Spring 2011

Doctoral Committee :

Department Chair: Simon Tavener

Adviser: Vakhtang Putkaradze

Simon Tavener
Patrick Shipman
Mario Marconi

ABSTRACT

CONSTRAINED DYNAMICS OF ROLLING BALLS AND MOVING ATOMS

This dissertation is devoted to the study of the dynamics, conservation laws and symmetries of rolling spheres, with special attention to applications to atomic and molecular systems. Previously known conservation laws of the rolling motion are associated with the nonholonomic version of Noether's theorem. Moreover, the conservation laws are related to the reduction by Lie symmetries of the dynamic equations of motion. Symmetries in the Noether's theorem and in the reduction by Lie symmetries are compared in their applications. In addition, we analyze the collective motion of the system of rolling particles for its statistical quantities under the constraint condition of rolling without slipping motion. The numerical simulations revealed some of qualitative characteristics in the statistical mechanics of the rolling-constrained system.

As a separate topic, the study of the molecular dynamics is discussed in relation to the results of recent experimental achievements with the non-contact atomic force microscopy. We propose a novel scenario explaining the process of single-atom manipulation in terms of the classical resonance effect.

ACKNOWLEDGEMENTS

I would like to express my gratitude and appreciation to my advisor Vakhtang Putkaradze who has been my thoughtful advisor and a good friend. His support and guidance has been the beacon for my journey in the ocean of science and mathematics. I also would like to thank my committee (Simon Tavener, Patrick Shipman and Mario Marconi) for reviewing this dissertation. I would like to thank Daniel Rudolph who was in my committee but passed away and is no longer with us. His passion and advice had been encouragement in my study. I would like to thank Darryl Holm (Imperial College London, UK) and Takashi Hikihara (Kyoto University, Japan) who introduced those fascinating topics in my work. They have been my mentors and good friends. We had much fun working together and their passions on science have inspired me a lot. I would like to thank Sunny Bak for giving the draft its first read and making many suggestions and corrections. Lastly, I would like to thank Masayuki Kimura and Cesare Tronci who I have met during my travel to get through this work.

TABLE OF CONTENTS

Chapter 1

INTRODUCTION

1.1 Outline

Dynamics in nature follow certain rules of order and symmetry. For example, the planets are orbiting around the sun in ordered and periodic manner and solid rocks have very regular lattice patterns in their atomic structures. The humans have admired such order and symmetry existing in nature for centuries and have been making great effort to understand its harmonic beauty. As a result, two interesting characteristics of the nature have been revealed; ordered, periodic and symmetric VS chaotic and unpredictable. The earth orbits around the sun in very regular and periodic manner as described by Newton, but at the same time, the orbital motion of planets is chaotic as revealed by Poincare. Atomic structure of diamond is very regular but the motion and distribution of electrons between the regular lattice of nuclei is very unpredictable and only probabilistic prediction is feasible.

In the effort of finding the nature as an ordered and predictable object, its symmetric characteristic has served as one of the most important features in understanding dynamics of the nature. Mathematical laws and orders are related to symmetries of the dynamics. The symmetries have been studied in several different directions

such as Lie group symmetry, reduction of order and conservation laws to name a few.

In an attempt to associate symmetries to conservation laws in the differential equations as the evolution model of dynamics, Emmy Noether first proved the relation between the symmetries of a dynamical system and the conservation laws of the system in the setting of variational problem. For example, energy conservation is related to the symmetry or, in other words, the invariance of the system under the time translation and the conservation of linear momentum can be the result of the invariance of the system under the linear translation. So, Noether's theorem has taught us that if a variational system was symmetric or invariant under a certain variation of the system, then the system would have the corresponding conservation law.

However, if the system of interest becomes constrained and non-variational, such association between the symmetry of the system and conservation law in the dynamics becomes unclear and the application of Noether's idea becomes a difficult issue. The topic of my study is about a type of constrained system of rigid body dynamics, *rolling rigid body*. The dynamics of rolling rigid body have found very useful applications in our daily lives. Automobiles and bicycles are all rolling on the ground. Learning how to balance and ride on a bicycle comes easy when learned during childhood, however, the dynamics of bicycles are not as easy as those of flying or sliding objects. One feature of such rolling motions is the constraint condition of rolling. The rolling condition imposes such condition that couples the translational and rotational motions of a moving body. Mathematically, nonholonomic constraint cannot be reduced to a function of coordinates only (holonomic constraint). People have studied such constrained dynamics of rigid

bodies. Some examples are the oval-shaped spinning toy, called the rattleback, or the round-shaped tippe top. Even in a simple form of a toy top, the unpredictable behavior in its dynamic motions can be shown. Many studies about the dynamics of such unintuitive motions have revealed valuable understanding about nonlinear dynamics and analytic solvability.

My study is focused on the nonholonomic system of rolling motion, named the Chaplygin's ball. The Chaplygin's ball is a spherical ball which rolls on the plane without slipping under the influence of gravity and the mass distribution could be arbitrary in the most general circumstance. The equation of motion would be nonlinear ordinary differential equation. The Chaplygin's ball is a rather simple dynamical system of rolling motion due to its spherical shape, and interestingly when the shape of the rolling object is generalized into a different shape, the dynamics become much more complicated. One of such motions is its direction reversing character when it's spined into one direction, it would stop spinning in that direction, but would rattle and then spin into the opposite direction. Even though such motion would be a very interesting problem, my study will focus on a simpler motion of Chaplygin's ball and will focus on the related conservation laws of its dynamics.

Several well-known conservation laws in the rolling motion of Chaplygin's ball are my primary interest in the first part of the dissertation. To summarize some of related conservation laws, the most general mass distribution of the rolling ball seems to allow only the conservation of the total energy since the constraint force due to the rolling condition does not do any work. However, if the mass is more symmetrically distributed on the ball, in other words, if the distribution is

cylindrical where two moments of inertia are equal, this rolling dynamics will allow more conservation laws known as the Jellett integral and the Routh integral. The Jellett integral and the Routh integral can be shown to be conserved quantities directly from the equation of motion, the cylindrical mass distribution plays an essential role in the derivation of conserved quantities. Chaplygin studied this case and understood that the system could be reduced and separated in the variables and eventually that the system could be integrated in this symmetric case [Cha02]. In the dynamics of the rolling symmetric Chaplygin's ball, the conservation laws could be strong indicators of certain symmetries of the system. And as demonstrated by Noether theorem in variational systems, we would expect to relate the conserved quantities with certain invariant transformations of the lagrangian of the rolling ball. Obviously the internal symmetry of the mass distribution should be essential for those conservation laws. But very interestingly, there seems to be no clear explanation on the symmetry actions that could be associated with the Jellett and Routh integrals [GN00]. Moreover even the form of the Routh integral has been considered as mysterious [BM02b, GN00]. Here my study seeks an application of the Noether theorem in its nonholonomic version to those well-known conservation laws.

After the study of dynamic equations and conservation laws of a single rolling ball was structured, we tried to make an application of such rolling motion into the dynamics of interacting rolling particles. We idealized the dynamics of water molecules in a monolayer on the silicon surface as the system of purely rolling particles. We studied the deterministic rolling motions using a computer simulation model. The dynamics of many rolling water molecules are analyzed in the view of the fundamental concepts in the statistical mechanics.

As a separate topic from the rolling motion, the atomic dynamics of controlling single atoms with the atomic force microscope (AFM) are discussed. In recent experiments, the atomic force microscopy has demonstrated many diverse controls of single atoms on the semiconductor surfaces, for example, the silicon surfaces. The state-of-art experiments have shown that we could manipulate the single atoms in many flexible ways. Based on the experimental results, we propose a new scenario explaining how those manipulation of single atoms are carried out. We propose that the manipulations are the results of the resonant effect of atomic vibrations under the interaction between the single target atom and the atoms in the AFM tip. In addition, the distortion in the field of potential energy around the target atom by the approach of the AFM tip can enhance the very localized manipulation of single atoms. In future work, we hope to confirm our proposed scenario of resonance in the experimental settings.

1.2 Law of motion

In classical dynamics of rigid bodies, the motion of a rigid body follows a certain governing law of nature and that law has been stated in several different manners. The first well-known statement is the Newton's law of motion.

Theorem 1.2.1 (Newton's law of motion)**.** *The motion of a rigid body in an absolute coordinate frame is governed by the following equations of motion,*

$$\frac{d^2(mx)}{dt^2} = F\,,$$
$$\frac{d(J\omega)}{dt} = T\,,$$

where m : mass, $J(t)$: the moment of inertia of the rigid body about its center of mass, $x(t)$: the position vector of the center of mass, $\omega(t)$: the angular velocity

of the body, F : the summed force and T : the summed torque about the center of mass of the body.

The Newton's law states that the linear translational motion of *the center of mass* (CM) is governed as the time derivative of the linear momentum vector ($m\dot{x}$) is equal to the external force and the time derivative of the angular momentum vector ($J\omega$) is equal to the external torque summed as acting on the CM of the body. This principle needs the exact understanding of the nature of external forces and torques acting on the rigid body.

The second popular description of dynamic law is the Hamilton's principle in Lagrangian mechanics. The Hamilton's principle requires the definition of Lagrangian of the system.

Definition 1.2.1 (Lagrangian)**.** *The Lagrangian of the system is the map from the phase space of the system to $\mathbb{R}$, $L : (q, \dot{q}, t) \to L(q, \dot{q}) \in \mathbb{R}$ and it is defined as*

$$L(q, \dot{q}, t) := \textit{kinetic energy} - \textit{potential energy}\,.$$

In this definition of the Lagrangian of a rigid body, the system variable q is the combination of the position vector of the CM and the rotation of the body. The rotation of the rigid body may be represented as $SO(3)$ matrix to describe the rotational orientation of the body in 3D space.

Definition 1.2.2 (Action integral)**.** *The action integral is a functional defined as*

$$S(q(t)) = \int_{t_1}^{t_2} L(q, \dot{q}, t)dt\,.$$

The second description of dynamic law of motion of rigid body is the Hamilton's principle.

Theorem 1.2.2 (Hamilton's principle)**.** *The motion of a rigid body is the extremal trajectory, $q(t)$, of the action integral between two specified states $q(t_1)$ and $q(t_2)$ as*

$$\delta S = \delta \left[\int_{t_1}^{t_2} L(q, \dot{q}, t) dt \right] = 0 \,.$$

The extremal trajectory $q(t)$ satisfies a second order differential equations which are called Euler-Lagrange equations.

Theorem 1.2.3. *The Euler-Lagrange equations are the equations for extremal trajectories of Hamilton's principle and can be given as*

$$\frac{d}{dt}\left(\frac{\partial L}{\partial \dot{q}}\right) - \frac{\partial L}{\partial q} = 0 \,.$$

Proof.

$$\begin{aligned} \delta S &= \int_{t_1}^{t_2} \delta(L(q, \dot{q}, t)) dt = \int_{t_1}^{t_2} < \frac{\partial L}{\partial q}, \delta q > + < \frac{\partial L}{\partial \dot{q}}, \delta \dot{q} > dt \\ &= - \int_{t_1}^{t_2} \left\langle \frac{d}{dt}\left(\frac{\partial L}{\partial \dot{q}}\right) - \frac{\partial L}{\partial q} dt, \delta q \right\rangle + \left[< \frac{\partial L}{\partial \dot{q}}, \delta q > \right]_{t_1}^{t_2} = 0 \,. \end{aligned}$$

The boundary condition gives $\delta q(t_1) = 0$ and the same at t_2. The arbitrary variation of δq will give the equations for extremal curve as the given Euler-Lagrange equations. □

The Newton's law and Hamilton's principle are equivalent when the force in Newton's law arises as a conservative force. A conservative force is such a force that arises as a gradient of a potential energy function. Hence if the force and torque arise from potential energies, the dynamic law of motion can be derived from either principle.

1.3 Lie group action in rigid body motion

The configurational space of rigid body motion consists of the translation of the CM and the rotation of the body about the CM. The translation can be easily represented by a position vector, but the representation of rotation is little cumbersome. There are several ways of representing a rotation of rigid body like Euler's angle, quaternion or $SO(3)$, special orthogonal matrix. Different representation of $SO(3)$ are equivalent, with each having its own advantages and disadvantages, and are still used commonly in different applications.
These different representations of rotation can be best described as Lie group and Lie group action on a manifold.

Definition 1.3.1 (Group)**.** *A group is a set of elements possessing a binary operation (composition) under which the set is closed, an identity element exists and each element has a unique inverse.*

Definition 1.3.2 (Lie group)**.** *A Lie group is a group that depends smoothly on a set of parameters. In other words, Lie group is a group that is also a finite-dimensional real smooth manifold.*

Rotational groups can be represented by $SO(3)$ matrices. And the group of rotations and translations is represented by the special Euclidean group, $SE(3)$ in 3 dimensions. The group $SE(3)$ can describe the rigid body motion in 3 dimensional space by its action on the configuration space of rigid motion.

Definition 1.3.3 (Group action)**.** *If G is a group and X is a set, then the (left) group action is the binary operation $G \times X \to X$, $g \cdot x \in X$ that satisfies*

- $(g \cdot h) \cdot x = g \cdot (h \cdot x)$ *, for all $g, h \in G$ and $x \in X$,*

- $e \cdot x = x$ *for all* $x \in X$ *and* e*, the identity element in* G*.*

Definition 1.3.4 (Semidirect-product Lie group)**.** *A Lie group* G *that may be decomposed uniquely into a normal subgroup* N *and a subgroup* H *such that every group element may be written as* $g = nh$ *or* $g = hn$ *(in either order) for unique choices of* $n \in N$ *and* $h \in H$ *is called a semidirect product of* H *and* N*, denoted in the present convention as* $G = H \ltimes N$*.*

The group $SE(3)$ is the semidirect-product of $SO(3)$ and $\mathbb{R}^3$; $SE(3) = SO(3) \ltimes \mathbb{R}^3$. And $SE(3)$ can serve for the configuration space of rigid body motion and its group action can be used for representation of the motion. The element of $SO(3)$ represents the rotation of a body and the element of $\mathbb{R}^3$ represents the translation of the CM of the body. The $SE(3)$ operation is defined as

$$(g_1, r_1) \cdot (g_2, r_2) = (g_1 \cdot g_2, g_1 \cdot r_2 + r_1)$$

where $g_{1,2} \in SO(3)$ and $r_{1,2} \in \mathbb{R}^3$. If the elements of $SO(3)$ are represented as 3×3 special orthogonal matrices, then the $SO(3)$ operation is simply the matrix multiplication and the $SO(3)$ action on $\mathbb{R}^3$ is the matrix-vector multiplication. Hence the product of $SO(3)$ element and $\mathbb{R}^3$ element belongs to $\mathbb{R}^3$ and $\mathbb{R}^3$ is the normal subgroup of $SE(3)$.

Definition 1.3.5 (Tangent bundle)**.** *If* M *is a smooth manifold, the tangent bundle,* TM *of* M *is the disjoint union of the tangent spaces of* M*,*

$$TM = \bigcup_{x \in M} T_x M \,.$$

When $SE(3)$ serves for the configuration space of the rigid body motion, then the phase space becomes the tangent bundle of $SE(3)$, which is noted as $TSE(3)$. An

element of the phase space becomes $(\dot{g}, \dot{r})_{(g,r)} \in TSE(3)$ where $(g, r) \in SE(3)$. Even though the phase space is the tangent bundle of $SE(3)$, the Lie algebra is more convenient tool for dealing with tangent space.

Definition 1.3.6 (Lie algebra)**.** *The Lie algebra* $\mathfrak{g}$ *of a Lie group* G *is the tangent space of the identity element of the Lie group.*

An element $\omega \in \mathfrak{g}$ can be represented as $g^{-1}\dot{g}$ or $\dot{g}g^{-1}$ depending on the left multiplication or right multiplication by the Lie group element. The Lie algebra is a vector space because it is the tangent space at the identity element and more over the Lie algebra is equipped with an extra binary operation which is called as the Lie bracket, $[\mathfrak{g}, \mathfrak{g}] \to \mathfrak{g}$. The Lie bracket operation is defined as a commutator operation, $[x, y] = x \cdot y - y \cdot x$, based on the Lie algebra multiplication which may not be closed in the Lie algebra. Once the multiplication of Lie algebra elements is defined, the Lie bracket has the following properties,

- $[x, y]$ is bilinear operation.
- $[x, x] = 0$ and $[x, y] = -[y, x]$.
- $[x, [y, z]] + [y, [z, x]] + [z, [x, y]] = 0$.

Hence the Lie bracket is anti-commutative bilinear operation which satisfies the Jacobi identity which is the third relation above.

The SE(3) group will be used to represent the configuration space of the rigid body motion and it also serves as the group of coordinate transformations acting on the configuration space.

Definition 1.3.7 (One-parameter group)**.** *A one-parameter group of transformations is the set of additive subgroup of G as*

$$g_{t_1+t_2} = g_{t_1} \cdot g_{t_2}$$

where $g_i \in G$ and " $\cdot$ " is the group operation.

If the one-parameter subgroup of a group G acts on a manifold M, then it generates a trajectory on M as

$$p(0) \in M \rightarrow p(t) = g(t) \cdot p(0) \in M\,,\ g(t) \in G\,.$$

Using the one-parameter subgroup, the trajectory of motion of a rigid body can be represented as the continuous action of the one-parameter subgroup on the initial configuration of the rigid body,

$$(h,p) \in SE(3) \rightarrow (g_t, r_t) \cdot (h,p) = (g_t \cdot h, g_t \cdot p + r_t) \in SE(3)$$
$$(g_t, r_t)|_{t=0} = Id \in SE(3).$$

Another way of obtaining Lie algebra element in $\mathfrak{g}$ of a group G is using differential operation on one-parameter subgroup,

$$\xi = \frac{d}{dt}(g(t))|_{t=0}\,,\ g(0) = Id \in G$$

Definition 1.3.8 (Vector field generated by Lie algebra)**.** *The action of Lie algebra, $\mathfrak{g}$ on the manifold M can generate a vector field as defined as*

$$\xi(p) = p(t)' = g(t)' \cdot p := \xi p\,,\ p \in M$$

where $g(t) \in G$ is a one parameter group such that $g(0) = Id$ and $g(t)'_{t=0} = \xi$.

These tools from Lie group can be used to describe the dynamics of rigid body motion. The coordinate transform between the body fixed frame and the spatially fixed frame is easily made.

$$\Omega(t) = g^{-1}\omega(t)g\,,$$
$$s(t) = g^{-1}\sigma\,,$$

where the first equation is the transform of angular velocity as 3×3 skew symmetric matrix and the second is the transform between 3 vectors. The relation between time derivatives of vector variables becomes also clear:

$$\begin{aligned}\frac{d}{dt}\sigma(t) &= \frac{d}{dt}(g(t)\cdot s(t)) = \dot{g}\cdot s + g\cdot\dot{s}\\ &\Rightarrow g^{-1}\cdot\frac{d}{dt}\sigma = \dot{s} + g^{-1}\dot{g}\cdot s = (\frac{d}{dt} + \Omega\times)s\,.\end{aligned}$$

Our work on deriving the equations of motion for rolling rigid body will use these operations and manipulations on variables in Lie group and Lie algebra, as represented by matrices or vectors.

1.4 Symmetries and conservation laws

Symmetries of a system of differential equations are the transformation of variables that leaves the system itself or a function related to the system invariant under the transformation.

Definition 1.4.1. *Lie symmetry is an invariance of the differential equations under continuous transformations.*

Such Lie symmetry group will transform a solution curve to another solution curve of the system.

Another type of symmetry is the Noether symmetry of a Lagrangian system.

Definition 1.4.2. *Noether symmetry is an invariance of the action integral of a Lagrangian system under the time and coordinate transformations.*

In Lagrangian mechanics, the Noether symmetry is associated with conservation laws of the equations of motion by the Noether's theorem.

Theorem 1.4.1 (Noether theorem)**.** *Each Noether symmetry of the action integral of a Lagrangian system corresponds to a constant of the motion.*

Chapter 2

ROLLING CHAPLYGIN'S BALL

Most previous theoretical studies assumed the rolling motion with a perfect friction, i.e., without slippage at the contact. Then such idealized dynamics have been studied for the equations of motion and their solution curves.

The resulting evolution equations are nonlinear system of differential equations and many analytic and numerical studies have been done. Analytic studies have focused on certain symmetric problems for its integrability, conservation laws or qualitative analysis like stability.

The most outstanding problem of rolling rigid body is the Chaplygin's ball. The Chaplygin's ball is a spherical ball that rolls without slipping on a horizontal plane (under gravity). The rigid body dynamics of a rolling ball show very interesting conservation laws under certain symmetric condition. In this chapter, we study the detail of the dynamics of Chaplygin's rolling ball and its conservation laws.

2.1 Equations of motion of rolling rigid body

The equations of motion for rolling rigid body had been a source of confusion and controversy and the correct equations of motion are now well understood and settled down. The correct equations of motion are derived by application of the Lagrange-d'Alembert principle.

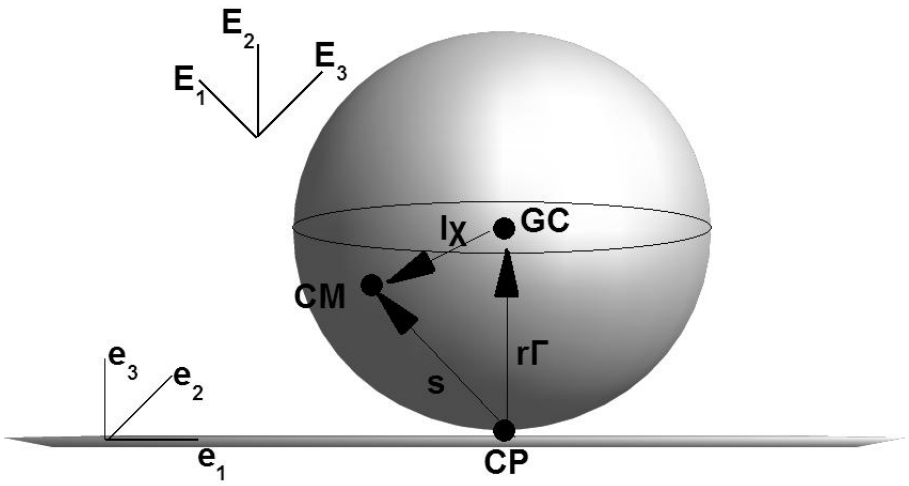

Figure 2.1: The schematic of the rolling ball

Theorem 2.1.1 (Lagrange-d'Alembert principle)**.** *If the constraint forces are orthogonal to all the allowable displacements consistent with the constraint, then the equations of motion for the constrained system can be given as*

$$\sum_i (F_i - m_i a_i) \cdot \delta r_i = 0$$

where F_i: applied forces, m_i: masses, a_i: acceleration of i-th mass and δr_i : virtual displacement consistent with the constraint.

Proof. The constraint force on i-th mass is $C_i = m_i a_i - F_i$ and the Lagrange-d'Alembert equations follow. □

The Lagrange-d'Alembert principle is applied to a constrained system and combining the Lagrange-d'Alembert equations and the given constraint conditions can determine the dynamics of the system. Hence the Lagrange-d'Alembert equations can serve as the law of dynamics as a generalized version of Newton's equation. The confusion about the correct equations of motion for a rolling ball comes from the fact that there could be more than two different trajectories of rolling motion

that satisfy the constraint of rolling condition and still conserve the total energy, which seems to satisfy the condition that the constraint force does no work. Some history of discussion about this confusion can be found in [Blo03, Koz92]. The incorrect equations of motion come when the rolling constraint is directly substituted into the Lagrangian to apply the variational principle for the Euler-Lagrange equations. The obtained Euler-Lagrange equations would satisfy the rolling constraint and would conserve the total energy of the rolling body, but it had been known to be incorrect equations of motion for the rolling rigid body.
In our discussion, we focus on the system of Chaplygin's rolling ball.

Definition 2.1.1 (Rolling constraint)**.** *The rolling without slipping constraint is given by a relation between the linear velocity of the CM and the angular velocity as*

$$\dot{x} = \omega \times \sigma \,, \text{ and in body-fixed moving frame, } V = \Omega \times s \,.$$

where $\dot{x}$: the translational velocity, ω: the spatial angular velocity, σ: the vector connecting the contact point and the CM and V , Ω , s are the same vectors as $\dot{x}$, ω , σ represented in the moving frame which is fixed on the CM.

The above rolling constraint is an equation between velocities and this condition cannot be integrated to make a constraint relation in configurational variables. Such type of constraint is called the nonholonomic constraint.

Definition 2.1.2 (Chaplygin's rolling ball)**.** *The Chaplygin's ball is the spherical body with offset center of mass moving with the perfect rolling constraint.*

We will use the vector notations as given in the figure (3.1). The vectors are given in the reference frame that is moving with the rolling ball and we will refer that

moving frame as *the body frame (E_i-frame) and in contrast, the absolute frame that is fixed on the plane will be referred as* the spatial frame (e_i-frame). Some of the vector notations in the spatial frame will be used as

- σ: the vector of s in spatial frame.
- $\dot{x}$, ω: the vectors of V , Ω respectively in spatial frame.

In this setting, $s = r\Gamma + \ell\chi$ where $\chi = E_3 = (0, 0, 1)^T$ and Γ is the normal unit vector to the plane of rolling in the moving frame which is fixed on the body.
we derive the equations of motion of rolling ball in two different approaches and compare them. Two different derivations will come from the Newtonian approach and the Lagrangian approach.

2.1.1 The equations of rolling ball in Newtonian mechanics

The derivation starts with Newton's equations with explicitly writing the constraint force and the constraint torque that are induced by the imposed rolling constraint.

$$\frac{d}{dt}(m\dot{x}) = F + N_c\,,$$
$$\frac{d}{dt}(J\omega) = T + T_c\,.$$

where F , T are the sum of applied forces and that of applied torques. And N_c , T_c are the constraint force and torque at the contact point. The m and J are the mass and the moment of inertia of the rolling ball. J is a symmetric 3 by 3 tensor which is normally a function of orientation of the body.

If there are no external force nor external torque applied on the rolling ball, then the constraint torque is induced only by the constraint force and we can use

$$T_c = (-\sigma) \times N_c \,,\; F = 0 \text{ and } T = 0 \,.$$

Then the equations for free rolling Chaplygin's ball can be obtained by the cancelation of N_c and by the rolling constraint, $\dot{x} = \omega \times \sigma$,

$$\begin{aligned} \frac{d}{dt}(m\dot{x}) &= N_c \,, \\ \frac{d}{dt}(J\omega) &= (-\sigma) \times \frac{d}{dt}(m\dot{x}) \,, \\ \frac{d}{dt}(J\omega) &= (-\sigma) \times \frac{d}{dt}(m\omega \times \sigma) \,. \end{aligned}$$

In the case of gravity force $(m\gamma)$ acting in $-e_3$ direction, the equations of rolling motion become

$$\frac{d}{dt}(J\omega) = (-\sigma) \times \left(\frac{d}{dt}(m\omega \times \sigma) - (-m\gamma e_3) \right) .$$

For the free rolling Chaplygin's ball, the complete system of equations in the spatial frame become

$$\dot{x} = \omega \times \sigma \,, \tag{2.1}$$

$$\frac{d}{dt}(J\omega) = (-\sigma) \times \frac{d}{dt}(m\omega \times \sigma) \,. \tag{2.2}$$

This system of equations can also be represented in the moving frame with the body,

$$V = \Omega \times s \,, \tag{2.3}$$

$$(\frac{d}{dt} + \Omega\times)(I\Omega) = (-s) \times ((\frac{d}{dt} + \Omega\times)(m\Omega \times s)) \,, \tag{2.4}$$

where I is the moment of inertia tensor in body frame and it is a constant tensor. If the body frame is aligned with the principal axes of inertia, then I becomes a

diagonal 3×3 tensor, $I = diag(I_1, I_2, I_3)$.

The equation (2.3) is the kinematic equation that is purely geometric and keep the ball rolling on the plane surface. But the equation (2.4) is the dynamic equation that is imposed by the relationship between the constraint force and torque at the contact point and it is purely deductive reasoning to use such a principle of motion and it needs to be confirmed in experiments. In [Koz92], Kozlov commented as "The question of the applicability of the non-holonomic model (indeed, like any other model of the mechanics of systems with constraints) cannot, in any specific situation be solved within the framework of an axiomatic scheme without recourse to the experimental results". Several experiments actually confirmed the validity of the dynamic equations [LM95].

2.1.2 The equations of rolling ball in Lagrangian mechanics

The equations of motion in Lagrangian mechanics come from the variational principle of least action. The actual trajectory of motion will become the extremal curve that minimizes the action integral between two specified end points in configurational space. However such application of variational principle to the Chaplygin's rolling ball is not straightforward due to the non-integrability of the non-holonomic rolling constraint.

Some usual situations in the least action principle are,

- the Lagrangian, $L = KE - PE$, contains all the forces in its potential energy,
- the holonomic constraints are applied to the Lagrangian and again, all the applied forces and constraint forces are contained in the form of potential energy.

Hence the application of variational derivative on the action integral and the Lagrangian will reproduce all the necessary forcing terms in the resulting Euler-Lagrange equations from the least action principle.

A troubling issue of applying the variational principle to the Chaplygin's rolling system is that the substitution of the rolling constraint into the Lagrangian doesn't generate the correct constraint force. This issue is the confusing one that had been a trouble at some time. However, the correct equations of motion come when the variational principle is twisted a little bit and this is exactly the application of the Lagrange-d'Alembert principle. So we apply the following procedure to modify the variational principle,

- -$\delta L := \frac{d}{dt}\left(\frac{\delta L}{\delta \dot{q}}\right) - \frac{\delta L}{\delta q} = (ma - F_{applied})$ is the constraint force,
- The actual constraint force can not be regenerated by the direct substitution of the nonholonomic constraint into the Lagrangian,
- use the Lie group and its action to represent the configurational space and the motion.

Considering these conditions, the correct equations of motion come as the Lagrange-d'Alembert equations.

Theorem 2.1.2 (Lagrange-d'Alembert equations)**.** *In the system of Chaplygin's free rolling ball, the following equations of motion are derived from the application of the Lagrange-d'Alembert principle,*

$$\frac{d}{dt}(J\omega) + \sigma \times (\frac{d}{dt}(m\omega \times \sigma)) = 0\,,\ \dot{x} = \omega \times \sigma \tag{2.5}$$

in the spatially fixed frame, and the same eqautions in the body frame are

$$(\frac{d}{dt}+\Omega\times)(I\Omega)+s\times((\frac{d}{dt}+\Omega\times)(m\Omega\times s))=0\,,\ V=\Omega\times s\,. \tag{2.6}$$

Proof. We begin with the variational derivative on the unconstrained Lagrangian of freely rolling ball,

$$\begin{aligned}\delta L &= \delta(\frac{1}{2}<J\omega,\omega>+\frac{1}{2}<m\dot{x},\dot{x}>)\\ &= \frac{1}{2}\left[<(\delta J)\omega+J\delta\omega>+<J\omega,\delta\omega>+<m\delta\dot{x},\dot{x}>+<m\dot{x},\delta\dot{x}>\right]\\ &= \frac{1}{2}\left[<(\delta J)\omega+J\delta\omega>+<J\omega,\delta\omega>\right]+<m\dot{x},\delta\dot{x}>\end{aligned}$$

where the notations are as followings,

- $J=g(t)Ig^{-1}(t)$ is the spatial moment of inertia tensor which is the 3×3 symmetric matrix and $g(t)\in SO(3)$ is the rotational trajectory of the rolling ball.
- $<A,B>:=tr(A^T\cdot B)$ is the matrix inner product for real valued matrices.
- $\omega\in so(3)$ is the angular velocity represented as 3×3 anti-symmetric matrix. (Same ω may represent a 3 vector for angular velocity. It should be clear by the context if ω is used as a 3 vector for an angular velocity.)

Now we go through individual variations and use the integration by parts with the fixed boundary condition. Some of the necessary details are

$$\begin{aligned}\delta(gg^{-1}) &= (\delta g)g^{-1}+g(\delta g^{-1})=0\rightarrow\ \delta g^{-1}\\ &= -g^{-1}\delta g g^{-1}\,,\\ \delta J &= \delta(gIg^{-1})=(\delta g)Ig^{-1}+gI(\delta g^{-1})=\delta g g^{-1}gIg^{-1}-gIg^{-1}\delta g g^{-1}\\ &= \delta g g^{-1}J-J\delta g g^{-1}\,,\\ \delta\omega &= \delta(\dot{g}g^{-1})=(\delta\dot{g})g^{-1}+\dot{g}(-g^{-1}\delta g g^{-1})=(\delta g g^{-1})\dot{}+(\delta g g^{-1}\dot{g}g^{-1}-\dot{g}g^{-1}\delta g g^{-1})\,,\\ \delta\dot{x} &= (\delta x)\dot{}\,.\end{aligned}$$

We use $\eta := \delta g g^{-1}$ for a variational angular velocity. Then we get

$$\begin{aligned}
\delta L &= \frac{1}{2} < (\eta J - J\eta)\omega, \omega > + < J\omega, \dot{\eta} + \eta\omega - \omega\eta > + < m\dot{x}, (\delta x)\dot{} > \\
&=< J\omega, \dot{\eta} > + < m\dot{x}, (\delta x)\dot{} > + \frac{1}{2}\left[tr\left\{\omega^T J^T \eta^T \omega - \omega^T \eta^T J^T \omega + 2\omega^T J^T (\eta\omega - \omega\eta)\right\}\right] \\
&=< J\omega, \dot{\eta} > + < m\dot{x}, (\delta x)\dot{} > + \frac{1}{2}\left[tr\left\{\omega J\eta\omega - \omega\eta J\omega - 2\omega J(\eta\omega - \omega\eta)\right\}\right] \\
&=< J\omega, \dot{\eta} > + < m\dot{x}, (\delta x)\dot{} >=< -\frac{d}{dt}(J\omega), \eta > + < -\frac{d}{dt}(m\dot{x}), \delta x >
\end{aligned}$$

where the value of trace operation becomes zero due to the property of trace operator. The fixed boundary condition for the variation is applied to make the integration by parts at the last part of the equation. And $\omega^T = -\omega\,,\ J^{=}J\,,\ \eta^T = -\eta$ and $tr(\omega J\omega\eta + \omega J\omega\eta) = tr(\omega J\omega\eta - \eta\omega J\omega) = tr(\omega J\omega\eta - \omega J\omega\eta) = 0$ is also used. Now we get,

$$\delta S = \int \delta L dt = \int < -(J\omega)\dot{}, \eta > + < -(m\dot{x})\dot{}, \delta x > dt \tag{2.7}$$

$$= \int < -(J\omega)\dot{}, \eta > + < -(m\omega \times \sigma)\dot{}, \eta \times \sigma > dt \tag{2.8}$$

$$= \int < -(J\omega)\dot{} - \sigma \times (m\omega \times \sigma)\dot{}, \eta > dt = 0 \tag{2.9}$$

and the arbitrariness of η brings the desired equations of motion as a form of Lagrange-d'Alembert equations.

$$(J\omega)\dot{} + \sigma \times (m\omega \times \sigma)\dot{} = 0\,,\ \text{with } \dot{x} = \omega \times \sigma\,.$$

In the equation (2.9) the rolling constraint is applied to make the variations to be consistent with the imposed rolling constraint, $\delta x = \eta \times \sigma$. This last step is the application of the Lagrange-d'Alembert principle and if there were no constraint, then the equations of free rigid body would have come from the equation (2.7).

Now the conversion into the equations in body frame can come from the conversion principle,

$$g^{-1}\frac{d}{dt}z = g^{-1}\left(\frac{d}{dt}(g\cdot Z)\right) = g^{-1}\dot{g}Z + g^{-1}g\frac{dZ}{dt} = \left(\frac{d}{dt} + \Omega\times\right)Z$$

where z and Z are the spatial and body representations of the same vector. □

2.1.3 Comparison of the equations of motion

Looking at the two different derivations of the equations of motion for the Chaplygin's rolling ball, we can see the application of the Lagrange-d'Alembert principle is much clearer in the Lagrangian mechanics. The dynamic principle for the freely rolling ball can be stated in two different ways in Newtonian and Lagrangian mechanics,

- Newtonian mechanics: the constraint torque is induced only by the constraint force.
- Lagrangian mechanics: the constraint force and torque are orthogonal to all the possibly allowable directions of motion.

The resulting equations for the free rolling ball are same. Hence the two above statements for the dynamic law of perfect rolling ball should be equivalent. However, the direct association is not that clear.

The second issue in the derivation of the equations is the application of the rolling constraint in the Lagrangian approach. In holonomically constrained systems, the constraint conditions are directly substituted into the Lagrangian and then the variational principle can be applied to arrive the equations of motion. We may

try the same strategy for the non-holonomic rolling constraint to get the reduced constrained Lagrangian,

$$L_c := \frac{1}{2}\left(< J\omega, \omega > + < m\omega \times \sigma, \omega \times \sigma >\right) ,$$

where the translational component has disappeared and the constrained Lagrangian is only a function of the rotation and the angular velocity, hence reducing the phase space to $TSO(3)$ from $TSE(3)$. Now if the variational derivative is taken on this constrained Lagrangian, we get the Euler-Lagrange equations.

$$\begin{aligned}
\delta L_c &= \delta\left[\frac{1}{2} < J\omega, \omega > + \frac{1}{2} < m\omega \times \sigma, \omega \times \sigma >\right] \\
&= < -(J\omega)^{\cdot}, \eta > + < m\omega \times \sigma, \delta\omega \times \sigma + \omega \times \delta\sigma > \\
&= < -(J\omega)^{\cdot}, \eta > + < m\omega \times \sigma, (\dot{\eta} + \eta \times \omega) \times \sigma + \omega \times (-\eta \times \ell\chi) > \\
&= < -(J\omega)^{\cdot}, \eta > \\
&+ < -\frac{d}{dt}(\sigma \times (m\omega \times \sigma)) + \omega \times (\sigma \times (m\omega \times \sigma)) + \ell\chi \times (\omega \times (m\omega \times \sigma)), \eta > \\
&= < -(J\omega)^{\cdot} - \sigma \times (m\omega \times \sigma)^{\cdot} + (\omega \times \ell\chi) \times (m\omega \times \sigma) \\
&+ \omega \times (\sigma \times (m\omega \times \sigma)) + \ell\chi \times (\omega \times (m\omega \times \sigma)), \eta >= 0
\end{aligned}$$

and the corresponding Euler-Lagrange equation is

$$\begin{aligned}
&(J\omega)^{\cdot} + \sigma \times (m\omega \times \sigma)^{\cdot} - (\omega \times \ell\chi) \times (m\omega \times \sigma) - \omega \times (\sigma \times (m\omega \times \sigma)) \\
&- \ell\chi \times (\omega \times (m\omega \times \sigma)) = 0 \,.
\end{aligned} \tag{2.10}$$

The problematic issue is that the resulting Euler-Lagrange equations, (2.10), are not the same equations as the Lagrange-d'Alembert equations, (2.5), of free rolling ball. Nonetheless, the dynamic evolution according to these Euler-Lagrange equations (2.10) is consistent with the rolling constraint and with the conservation of

the total energy of the system. Hence even along this *incorrect* trajectory, the constraint force is not doing any work on the system.

Thus the Lagrange-d'Alembert equations and the Euler-Lagrange equations are not the same in the rolling dynamics of Chaplygin's ball. Then what can be the geometric interpretation of the constraint force and torque in the correct Lagrange-d'Alembert equations, (2.5), for the Chaplygin's rolling ball? The answer has been studied in the context of *Ehresmann connection* ([Blo03]) and the discrepancy between the equations (2.10) and (2.5) is coming from the curvature of the associated Ehresmann connection.

2.1.4 Conservation laws and symmetries in Chaplygin's rolling ball

For general mass distribution in the Chaplygin's ball, it is not known if there is any conserved quantity along the motion other than the total energy conservation. However, there appear two more conserved quantities along the motion if the mass distribution of the rolling ball satisfies certain symmetry conditions, which will be called as cylindrically symmetric Chaplygin's ball. The symmetry conditions are as follows:

- The moment of intertia is symmetric about a principal axis. For the representation of the moment of inertia in its diagonal form, this condition states $I_1 = I_2 \neq I_3$. I_3 may be equal to the other components of the principal moment of inertia, but it is not required for the symmetry of our concern.

- The center of mass (CM) of the ball is located along the symmetry axis. So in the body frame of principal axes, $\chi = E_3$ and thus the mass distribution of the ball becomes cylindrically symmetric. The CM may coincides with the geometric center (GC), but it is not required.

Satisfying these two conditions for the symmetric imbalanced Chaplygin's ball, there appear two extra prominent conservation laws and the rolling motion of a symmetric imbalanced ball had been proved to be analytically integrable by a Russian mathematician, Chaplygin. The two conservation laws are called as Jellett and Routh integrals and they are given as their representation in the body frame for the free rolling ball (no external field other than constraining with the rolling without slipping condition).

$$J =< I\Omega, s >= rI_1(\Omega_1\Gamma_1 + \Omega_2\Gamma_2) + I_3\Omega_3(r\Gamma_3 + \ell)\,,$$
$$R = \Omega_3\sqrt{I_1I_3 + m < Is, s >} = \Omega_3\sqrt{I_1I_3 + m(I_1r^2\Gamma_1^2 + I_1r^2\Gamma_2^2 + I_3(r\Gamma_3 + \ell)^2)}\,.$$

Actually these two conservation laws are preserved for the presence of an external gravity field in the normal direction to the plane of rolling. However, we will focus mainly on the free rolling motion under no external potential field to simplify the problem without eliminating the feature of prominent conservation laws of Jellett and Routh.

The physical interpretation of the Jellett and Routh integrals is not fully understood yet and the symmetry origins for the conservation laws are still confusing. Hence, my discussion will focus on the two conservation laws and on possible association of symmetry to those conservation laws.

To my knowledge, the Routh integral has not been studied in the association with a symmetry action in the context of Noether's theorem. My study tries to modify the Noether's theorem into the nonholonomic system and find its application to the conservation law of Routh integral.

2.2 Noether's theorem in symmetric Chaplygin's rolling ball

In variational problem, the Noether's theorem provides the association between conservation laws and symmetries. Similar association can be made in the problem of rolling ball with its Lagrange-d'Alembert equations. Basically, the two prominent conserved quantities of the Routh and Jellett's integrals can be associated to their corresponding infinitesimal variations. We will work out the variations in the body frame.

$$
\begin{aligned}
\delta L &= < I\Omega, \delta\Omega > + < mV, \delta V > , \\
\delta\Omega &= \delta(g^{-1}\dot{g}) = -g^{-1}\delta g g^{-1}\dot{g} + g^{-1}\delta\dot{g} = (g^{-1}\delta g)^{\cdot} + g^{-1}\dot{g}g^{-1}\delta g - g^{-1}\delta g g^{-1}\dot{g} \\
&= \dot{\eta} + [\Omega, \eta] , \\
\delta V &= \delta(g^{-1}\dot{x}) = -g^{-1}\delta g g^{-1}\dot{x} + g^{-1}\delta\dot{x} = (g^{-1}\delta x)^{\cdot} + g^{-1}\dot{g}g^{-1}\delta x - g^{-1}\delta g g^{-1}\dot{x} \\
&= (\eta \times s)^{\cdot} + [\Omega, \eta]s .
\end{aligned}
$$

The nonholonomic variation is applied by taking the variation first $\delta\dot{x} = (\delta x)^{\cdot}$ and then applying the rolling constraint $(\delta x)^{\cdot} = (\eta \times s)^{\cdot}$. With this careful step of taking variational derivative, the correct Lagrange-d'Alembert equations follow as the equations of motion by the vanishing $\delta S = 0$ for the arbitrary η with fixed boundary condition.

The Noether's theorem is applied to this nonholonomic variation in the following manner,

$$
\begin{aligned}
\delta L =& < I\Omega, \delta\Omega > + < mV, \delta V > \\
=& < I\Omega, \dot{\eta} + \Omega \times \eta > + < mV, (\eta \times s)\dot{} + (\Omega \times \eta) \times s > \\
=& - < (\frac{d}{dt} + \Omega\times)(I\Omega) + s \times ((\frac{d}{dt} + \Omega\times)(m\Omega \times s)), \eta > \\
&+ \frac{d}{dt}(< I\Omega, \eta > + < s \times mV, \eta >) \\
=& \frac{d}{dt}(< I\Omega, \eta > + < s \times mV, \eta >) = \frac{d}{dt}(< I\Omega + s \times m(\Omega \times s), \eta >) .
\end{aligned}
$$

In the application of the Noether's theorem, several things are assumed. These conditions will distinguish the application of the least action principle and that of the Noether's theorem in nonholonomic system.

- $\Omega(t)$ and $s(t)$ are the solution trajectory of the motion equations given as the Lagrange-d'Alembert equations.
- The variations of $\delta\Omega$ and δV are induced by the change of coordinate system, which is consistent with the rolling constraint. Hence the variation δV is taken with first applying the variational derivative and then the rolling constraint applied.
- The fixed endpoints condition is not applied as in the least action principle because the variation is induced by the time and coordinate transformation for applying Noether's theorem.

And we get a version of Noether's theorem in the Chaplygin's rolling ball.

Theorem 2.2.1 (Nonholonomic Noether's theorem)**.** *If the Lagrangian is invariant under an infinitesimal coordinate variation that is consistent with the rolling constraint, then there is a corresponding conservation law given as,*

$$
\delta L = \frac{d}{dt}(< I\Omega + s \times (m\Omega \times s), \eta >) = 0
$$

$$< I\Omega + s \times (m\Omega \times s), \eta >= constant$$

where $\eta \in so(3)$ *is angular velocity for the infinitesimal coordinate variation.*

This version is applied to the two prominent conservation laws in the case of cylindrically symmetric, imbalanced rolling ball.

$$J =< I\Omega + s \times (m\Omega \times s), s >=< I\Omega, s > , \tag{2.11}$$
$$R =< I\Omega + s \times (m\Omega \times s), \frac{I_1\chi + m < s, \chi > s}{\sqrt{I_1 I_3 + m < Is, s >}} > \ .$$

Just looking at the Lagrangian, $L = (< I\Omega, \Omega > + < m\Omega \times s, \Omega \times s >)/2$, this Lagrangian is invariant under any translational and any rotational coordinate transformation if the coordinate transformation in Noether's theorem is assumed as free of any constraint. Hence the Noether's theorem provides the association between such invariance and the conservations of linear and angular momentums in free body motion. However, such linear and angular momentums are not conserved in the rolling free body and there are the Jellett and Routh integrals instead.
Since the geometry of the plane of rolling motion and the internal symmetry of the ball about the symmetric axis indicate good possibility of symmetries, we can assume that the Γ and χ vectors are the axes of symmetry and try to seek the symmetry as the rotation about these vectors.

Example 2.2.1

If $\eta = \Gamma$ which is the infinitesimal variation as the rolling about the normal vector to the plane,

$$\delta\Omega|_{\eta=\Gamma} = \dot{\Gamma} + \Omega \times \Gamma = -\Omega \times \Gamma + \Omega \times \Gamma = 0 \,,$$
$$\delta V|_{\eta=\Gamma} = (\Gamma \times s)^{\cdot} + (\Omega \times \Gamma) \times s = (-\Omega \times \Gamma) \times \ell\chi + (\Omega \times \Gamma) \times s = (\Omega \times \Gamma) \times r\Gamma \,,$$
$$\delta L|_{\eta=\Gamma} =< I\Omega, \delta\Omega > + < m\Omega \times s, \delta V >= 0 + < m\Omega \times s, (\Omega \times \Gamma) \times r\Gamma >$$
$$=< \Omega, r\Gamma > \cdot < m\Omega \times \ell\chi, \Gamma >\neq 0 \,,$$

where $\dot{s} = (r\Gamma + \ell\chi)^{\cdot} = -\Omega \times r\Gamma$ is used. Hence $\delta L \neq 0$ brings that $\eta = \Gamma$ doesn't induce a conservation law by the Noether's theorem.

□

Example 2.2.2

If $\eta = \chi$ which is the axis vector of internal symmetry of the body and also a constant vector in the body frame,

$$\begin{aligned}
\delta\Omega|_{\eta=\chi} &= \dot{\chi} + \Omega \times \chi = \Omega \times \chi\,, \\
\delta V|_{\eta=\chi} &= (\chi \times s)^{\cdot} + (\Omega \times \chi) \times s = \chi \times (-\Omega \times r\Gamma) + (\Omega \times \chi) \times s\,, \\
\delta L|_{\eta=\chi} &=< I\Omega, \delta\Omega > + < m\Omega \times s, \delta V >=< I\Omega, \Omega \times \chi > \\
&\quad + < m\Omega \times s, \chi \times (-\Omega \times r\Gamma) + (\Omega \times \chi) \times s > \\
&\quad = 0 + < m\Omega \times s, < \chi, \Omega > r\Gamma + < \Omega, s > \chi > \\
&\quad =< \Omega, r\Gamma > \cdot < m\Omega \times r\Gamma, \chi >\neq 0\,.
\end{aligned}$$

Hence $\delta L \neq 0$ indicates that $< I\Omega + s \times (m\Omega \times s), \chi >$ is not a conservation law. □

Example 2.2.3

If $\eta = s = r\Gamma + \ell\chi$, then the variation of the Lagrangian comes from the linear combination of the previous two examples,

$$\begin{aligned}
\delta L|_{\eta=s} &= r\delta L|_{\eta=\Gamma} + \ell\delta L|_{\eta=\chi} \\
&\quad = r < \Omega, r\Gamma > \cdot < m\Omega \times \ell\chi, \Gamma > + \ell < \Omega, r\Gamma > \cdot < m\Omega \times r\Gamma, \chi >= 0
\end{aligned}$$

and the associated conserved quantity is the Jellett integral, $J =< I\Omega + s \times (m\Omega \times s), s >=< I\Omega, s >$. □

Example 2.2.4

If η is given as an angular velocity vector as

$$\eta = \frac{I_1\chi + m < s, \chi > s}{\sqrt{I_1 I_3 + m < Is, s >}},$$

then $\delta L = 0$ and the Routh integral is another conservation law. This can be checked with direct calculation of $\delta\Omega$ and δV. $\square$

Proof. We use a simplifying notation for the vector η,

$$\eta = a\chi + bs\,,\ s = r\Gamma + \ell\chi$$
$$a = \frac{I_1}{\sqrt{I_1 I_3 + m < Is, s >}}\,,\ b = \frac{m < s, \chi >}{\sqrt{I_1 I_3 + m < Is, s >}}$$

Then the variations are:

$$\delta\Omega = \dot{\eta} + \Omega \times \eta = \dot{a}\chi + \dot{b}s + b\dot{s} + \Omega \times (a\chi + bs)\,,$$
$$\delta V = ((a\chi + bs) \times s)\dot{} + (\Omega \times (a\chi + bs)) \times s$$
$$= \dot{a}\chi \times s + a\chi \times \dot{s} + (\Omega \times (a\chi + bs)) \times s\,,$$
$$\dot{a} = \frac{I_1 m < Is, \Omega \times r\Gamma >}{(I_1 I_3 + m < Is, s >)^{3/2}}\,,$$
$$\dot{b} = \frac{m < -\Omega \times r\Gamma, \chi > (I_1 I_3 + m < Is, s >) + m^2 < s, \chi >< Is, \Omega \times r\Gamma >}{(I_1 I_3 + m < Is, s >)^{3/2}}$$

and we use vector identities

$$< A, B \times C > = < B, C \times A > = < C, A \times B >\,,$$
$$(A \times B) \times C + (B \times C) \times A + (C \times A) \times B = 0\,,$$
$$A \times (B \times C) = < A, C > B - < A, B > C\,.$$

And the internal cylindrical symmetry of $I = diag(I_1, I_1, I_3)$, $\chi = E_3 = (0,0,1)^T$ gives another identity

$$< I\Omega, \Omega \times \chi >=< \Omega \times I\Omega, \chi >= 0\,.$$

Now using these identities and notations,

$$\begin{aligned}
\delta L =& < I\Omega, \dot{a}\chi + \dot{b}s + b\dot{s} + \Omega \times (a\chi + bs) > \\
&+ < m\Omega \times s, \dot{a}\chi \times s + a\chi \times \dot{s} + (\Omega \times (a\chi + bs)) \times s > \\
&=< I\Omega, \dot{a}\chi + \dot{b}s + b(-\Omega \times r\Gamma) + \Omega \times a\chi + b\Omega \times s > \\
&+ < m\Omega \times s, \dot{a}\chi \times s + a\chi \times (-\Omega \times r\Gamma) + < \Omega, s > (a\chi + bs) - < a\chi + bs, s > \Omega > \\
&=< I\Omega, \dot{a}\chi + \dot{b}s > + < m\Omega \times s, \dot{a}\chi \times s + < a\chi, \Omega > r\Gamma \\
&- < a\chi, r\Gamma > \Omega + < \Omega, s > a\chi > \\
&=< I\Omega, \dot{a}\chi + \dot{b}s > + < m\Omega \times s, \dot{a}\chi \times s + < \Omega, r\Gamma > a\chi > \\
&= \dot{a}(< I\Omega, \chi > + < s \times (m\Omega \times s), \chi >) + \dot{b} < I\Omega, s > \\
&+ < \Omega, r\Gamma >< m\Omega \times r\Gamma, a\chi > \\
&= \frac{I_1 m < Is, \Omega \times r\Gamma >}{(I_1 I_3 + m < Is, s >)^{3/2}}(< I\Omega + m|s|^2\Omega, \chi > -m < \Omega, s >< s, \chi >) \\
&+ \frac{m < -\Omega \times r\Gamma, \chi > (I_1 I_3 + m < Is, s >) + m^2 < s, \chi >< Is, \Omega \times r\Gamma >}{(I_1 I_3 + m < Is, s >)^{3/2}} < I\Omega, s > \\
&+ \frac{(I_1 I_3 + m < Is, s >) m I_1 < \Omega, r\Gamma >< \Omega \times r\Gamma, \chi >}{(I_1 I_3 + m < Is, s >)^{3/2}} \\
&= \frac{(I_1 I_3 + m < Is, s >) m}{(I_1 I_3 + m < Is, s >)^{3/2}}\{< -\Omega \times r\Gamma, \chi >< I\Omega, s > + I_1 < \Omega, r\Gamma >< \Omega \times r\Gamma, \chi >\} \\
&+ \frac{m < Is, \Omega \times r\Gamma >}{(I_1 I_3 + m < Is, s >)^{3/2}}\{I_1(< I\Omega + m|s|^2\Omega, \chi > -m < \Omega, s >< s, \chi >) \\
&+ m < s, \chi >< I\Omega, s >\} \\
&= \frac{(I_1 I_3 + m < Is, s >) m}{(I_1 I_3 + m < Is, s >)^{3/2}}\{r(\Omega_1\Gamma_2 - \Omega_2\Gamma_1)(I_1 r\Gamma_3 - I_3(r\Gamma_3 + \ell))\Omega_3\} \\
&+ \frac{-mr(\Omega_1\Gamma_2 - \Omega_2\Gamma_1)(I_1 r\Gamma_3 - I_3(r\Gamma_3 + \ell))}{(I_1 I_3 + m < Is, s >)^{3/2}}\{(I_1 I_3 + m < Is, s >)\Omega_3\} \\
&= 0\,.
\end{aligned}$$

Hence even for

$$\eta = \frac{I_1\chi + m < s, \chi > s}{\sqrt{I_1 I_3 + m < Is, s >}},$$

the variation of the Lagrangian δL vanishes and the nonholonomic Noether's theorem applies to the Routh integral with η as specified. □

A nonholonomic version of the Noether's theorem is successfully applied to the conservation laws of Jellett and Routh integrals. And the original form of the Routh integral was

$$R = \Omega_3 \sqrt{I_1 I_3 + m < Is, s >}$$

and this mysterious form of the conservation law is brought into a new form which corresponds to the nonholonomic Noether's theorem. And the nonholonomic Noether's theorem can be applied to the energy conservation of $H =< I\Omega + s \times (m\Omega \times s), \Omega > /2$ where the symmetry vector $\eta = \Omega$.

However, even with such successful application of Noether's theorem to conservation laws, we still do not fully understand the conservation laws of the symmetric rolling boll. Some of the fundamental questions could be

1. What could be the physical interpretations (or interpretation of the related symmetries) of the Jellett and Routh integrals?

2. How could the symmetric variation vector η be found for the symmetry of the rolling dynamics with Jellett and Routh integrals?

3. How could the conservation laws be found in such nonholonomic dynamics?

4. If the coordinate system moves by $\eta = \Omega$ which is the symmetry vector for the energy conservation, the coordinate system becomes the body frame. Now

if the coordinate system moves by other symmetry vectors of η for Jellett and Routh integrals, could there be any special feature in using such moving frames which evolve with corresponding η and looking at the dynamics in those moving frames?

On the last question above, those symmetric variational actions related to the Jellett, the Routh and the energy integrals are such coordinate transformations that preserve the as value of Lagrangian in their own moving frames as that of the absolute spatially fixed frame, thus the trajectories of rolling motion will be identical if they are derived as the extremal curves in the nonholonomic variational principle. Hence it seems that those symmetry coordinates of moving frames are special because they preserve the same dynamics of the rolling motion. More study in this perspective may be an interesting future problem.

Even though the nonholonomic Noether's theorem is successful in associating the invariant variations of the Lagrangian with the Jellett and Routh integrals, nothing is yet clearly understood. Nonetheless, such mystery of conservation laws in symmetric rolling ball is strongly believed to allow its understanding in the connection with symmetries as many other physical conservation laws have been understood in such way.

2.3 Symmetry reduction in symmetric Chaplygin's rolling ball

2.3.1 Symmetric unbalanced Chaplygin's rolling ball under no gravity (free rolling ball)

Sophus Lie(1842) introduced continuous symmetry groups to solve nonlinear differential equations and such tool of using Lie group and Lie algebra in solving differential equations became very strong analytic method. Here we use the tool of

reducing the order of a system of differential equations using Lie group symmetries. The detailed process is nicely explained in the textbook ([Olv93]) by P. Olver and here we follow the same tools as explained in the reference.

We already know there are several conservation laws for the dynamics of a cylindrically symmetric Chaplygin's ball, however the symmetry origin is not very straightforward. The only symmetry is the symmetric internal mass distribution, but the detailed connection to the conservation laws had not been clearly understood yet. Chaplygin himself already proved that the symmetric ball's rolling dynamics are completely integrable, so we focus on the detailed work on the reduction process by seemingly evident Lie symmetries in the equations of motion. Inspecting the equations of motion, we can find Lie symmetries of the differential equations of rolling motion.

We can inspect such Lie symmetries on the equations of motion in the body frame which is moving frame with the body. Then the cylindrical mass distribution imposes certain symmetry features into the system of equations. These symmetries are: invariances under rotation, time translation and scaling of angular velocity vectors in the system of symmetric and imbalanced rolling ball's motion. As a simpler problem, we start with cylindrically symmetric imbalanced free-rolling ball under zero gravity, $\ell \neq 0\,,\ I_1 = I_2 \neq I_3$. The reduction by symmetry in solving a system of differential equations can be extended to include non-zero gravity field in Chaplygin's rolling ball and the Jellett and Routh integrals are still conserved quantities in such an extension.

The explicit equations of motion are as follows.

$$
\begin{aligned}
&(\frac{d}{dt} + \Omega\times)(I\Omega) + s \times ((\frac{d}{dt} + \Omega\times)(m\Omega \times s)) = 0\,, \\
&\dot{\Gamma} = -\Omega \times \Gamma\,,\ V = \Omega \times s \\
&\Rightarrow \\
&(I_1 + m(r^2+\ell^2) + 2mr\ell\Gamma_3)\dot{\Omega}_1 - mr^2(\dot{\Omega}_1\Gamma_1 + \dot{\Omega}_2\Gamma_2 + \dot{\Omega}_3(\Gamma_3 + \ell/r))\Gamma_1 \qquad (2.12) \\
&= -mr\ell(-\Omega_1\Gamma_2 + \Omega_2\Gamma_1)\Omega_1 + mr\ell(\Omega_1\Gamma_1 + \Omega_2\Gamma_2 + \Omega_3(\Gamma_3 + \ell/r))\Omega_2 \\
&+ (I_1 - I_3)\Omega_2\Omega_3\,, \\
&(I_1 + m(r^2+\ell^2) + 2mr\ell\Gamma_3)\dot{\Omega}_2 - mr^2(\dot{\Omega}_1\Gamma_1 + \dot{\Omega}_2\Gamma_2 + \dot{\Omega}_3(\Gamma_3 + \ell/r))\Gamma_2 \\
&= -mr\ell(-\Omega_1\Gamma_2 + \Omega_2\Gamma_1)\Omega_2 - mr\ell(\Omega_1\Gamma_1 + \Omega_2\Gamma_2 + \Omega_3(\Gamma_3 + \ell/r))\Omega_1 \\
&- (I_1 - I_3)\Omega_1\Omega_3\,, \\
&(I_3 + m(r^2+\ell^2) + 2mr\ell\Gamma_3)\dot{\Omega}_3 - mr^2(\dot{\Omega}_1\Gamma_1 + \dot{\Omega}_2\Gamma_2 + \dot{\Omega}_3(\Gamma_3 + \ell/r))(\Gamma_3 + \ell/r) \\
&= -mr\ell(-\Omega_1\Gamma_2 + \Omega_2\Gamma_1)\Omega_3\,, \\
&\dot{\Gamma}_1 = -\Omega_2\Gamma_3 + \Omega_3\Gamma_2\,, \\
&\dot{\Gamma}_2 = -\Omega_3\Gamma_1 + \Omega_1\Gamma_3\,, \\
&\dot{\Gamma}_3 = -\Omega_1\Gamma_2 + \Omega_2\Gamma_1
\end{aligned}
$$

This system of equations is already reduced by the constraint condition and the equations are the evolution equations for the rotational motion of the rolling ball. This system is closed system between variables of Ω and Γ. To compute the translational motion, we can use the reconstruction equations as

$$
\begin{aligned}
V = g^{-1}\dot{x} = \Omega \times s\,, \\
\dot{x} = g(t)V\,.
\end{aligned}
$$

Hence the translational trajectory of $x(t) \in \mathbb{R}^3$ can be integrated once the solution of rotation $g(t) \in SO(3)$ is solved. Thus the symmetry reduction will be only

applied to the above system of equations for the angular motion.

The obvious symmetry actions from inspection of the equations are as follow.

$$\text{Rotation} : (\Omega_1, \Omega_2) \to (\Omega_1 \cos\epsilon + \Omega_2 \sin\epsilon, -\Omega_1 \sin\epsilon + \Omega_2 \cos\epsilon),$$
$$(\Gamma_1, \Gamma_2) \to (\Gamma_1 \cos\epsilon + \Gamma_2 \sin\epsilon, -\Gamma_1 \sin\epsilon + \Gamma_2 \cos\epsilon).$$
$$\text{Time translation} : t \to t + \epsilon\,,\ \Omega \to \Omega\,,\ \Gamma \to \Gamma\,.$$
$$\text{Scaling} : \Omega \to e^{\epsilon}\Omega\,,\ t \to e^{-\epsilon}t\,,\ \Gamma \to \Gamma\,.$$

And the unusual conservation laws of Jellett and Routh integrals are given as

$$J =< I\Omega, s >= r(I_1\Omega_1\Gamma_1 + I_1\Omega_2\Gamma_2 + I_3\Omega_3(\Gamma_3 + \ell/r))\,,$$
$$R = \Omega_3\sqrt{I_1I_3 + m < Is, s >} = \Omega_3\sqrt{I_1I_3 + mr^2(I_1\Gamma_1^2 + I_1\Gamma_2^2 + I_3(\Gamma_3 + \ell/r)^2}\,.$$

Now we would like to see the relation between the existing Lie symmetries of the system of equations and the unusual conservation laws on Jellett and Routh. For this purpose we proceed with the reduction of order applying the Lie symmetries. The invariance of the system of differential equations under the given symmetry transforms can be directly checked with the given system. For example, the rotation symmetry can be confirmed under the following change of variables,

$$\tilde{\Gamma}_1 = \cos\epsilon\Gamma_1 + \sin\epsilon\Gamma_2\,,$$
$$\tilde{\Gamma}_2 = -\sin\epsilon\Gamma_1 + \cos\epsilon\Gamma_2\,,$$
$$\tilde{\Omega}_1 = \cos\epsilon\Omega_1 + \sin\epsilon\Omega_2\,,$$
$$\tilde{\Omega}_2 = -\sin\epsilon\Omega_1 + \cos\epsilon\Omega_2\,,$$
$$\tilde{\Gamma}_3 = \Gamma_3\,,$$
$$\tilde{\Omega}_3 = \Omega_3\,.$$

With this change of variables by rotation about E_3 axis, the system in new variables is exactly the same system as (2.12).

Thus the symmetry transforms are Lie symmetries that transform solution curves to another solution curves of the system of differential equations. We follows the application of symmetries as in [Olv93], and reduce the system in sequential applications of symmetries.

We can start the symmetry reduction with the rotational symmetry first. For the reduction, we find a variable that straighten the symmetry action and invariant variables under the symmetry action. The variable that explicitly straighten the rotational symmetry action is the angle, θ, which will be called as explicit action variable from now on. The original system of equations will be transformed into:

$$\frac{d\theta}{dt} = \frac{d}{dt}\left(\tan^{-1}(\frac{\Gamma_2}{\Gamma_1})\right) = \frac{\dot{\Gamma}_2\Gamma_1 - \dot{\Gamma}_1\Gamma_2}{\Gamma_1^2+\Gamma_2^2} = \frac{-(\Gamma_1^2+\Gamma_2^2)\Omega_3 + (\Omega_1\Gamma_1+\Omega_2\Gamma_2)\Gamma_3}{\Gamma_1^2+\Gamma_2^2}$$

The *reduced* system of equations for invariant variables are obtained from the original system. The invariant variables under symmetry rotation are

$$\Gamma_3\,,\ \Omega_3\,,\ (\Omega_1\Gamma_1+\Omega_2\Gamma_2)\,,\ (\Omega_1^2+\Omega_2^2)\,, \tag{2.13}$$

and $-\Omega_1\Gamma_2+\Omega_2\Gamma_1$ is a function of the invariant variables and so is $\Gamma_1^2+\Gamma_2^2 = 1-\Gamma_3^3$.

$$-\Omega_1\Gamma_2+\Omega_2\Gamma_1 = (+/-)\sqrt{(\Omega_1^2+\Omega_2^2)(\Gamma_1^2+\Gamma_2^2)-(\Omega_1\Gamma_1+\Omega_2\Gamma_2)^2}$$

where the sign is determined by the initial condition for the system and we will just assume the positive sign without loss of generality.

Now $\Omega_1\dot{\Gamma}_1 + \Omega_2\dot{\Gamma}_2 = -\Omega_3(-\Omega_1\Gamma_2 + \Omega_2\Gamma_1)$ is used to make the following system.

$$
\begin{aligned}
&\frac{d\Gamma_3}{dt} = -\Omega_1\Gamma_2 + \Omega_2\Gamma_1 = \sqrt{(\Omega_1^2+\Omega_2^2)(\Gamma_1^2+\Gamma_2^2) - (\Omega_1\Gamma_2+\Omega_2\Gamma_2)^2}\,,\\
&(I_3 + mr^2 - mr^2\Gamma_3^2)\frac{d\Omega_3}{dt} - mr^2(\Gamma_3+\ell/r)\frac{d(\Omega_1\Gamma_1+\Omega_2\Gamma_2)}{dt} = mr^2\Gamma_3\Omega_3(-\Omega_1\Gamma_2+\Omega_2\Gamma_1)\,,\\
&- mr^2(1-\Gamma_3^2)(\Gamma_3+\ell/r)\frac{d\Omega_3}{dt} + (I_1 + m\ell^2 + mr^2\Gamma_3^2 + 2mr\ell\Gamma_3)\frac{d(\Omega_1\Gamma_1+\Omega_2\Gamma_2)}{dt}\\
&= -\Omega_3(-\Omega_1\Gamma_2+\Omega_2\Gamma_1)(I_1 + mr^2\Gamma_3^2 + mr\ell\Gamma_3 + I_3 - I_1)\,,\\
&(I_1 + m(r^2+\ell^2) + 2mr\ell\Gamma_3)\frac{d(\Omega_1^2+\Omega_2^2)}{dt}\\
&- 2mr^2(\Omega_1\Gamma_1+\Omega_2\Gamma_2)\left(\frac{d(\Omega_1\Gamma_1+\Omega_2\Gamma_2)}{dt} + (\Gamma_3+\ell/r)\frac{d\Omega_3}{dt}\right)\\
&= 2mr^2\Omega_3(-\Omega_1\Gamma_2+\Omega_2\Gamma_1)(\Omega_1\Gamma_1+\Omega_2\Gamma_2) - 2mr\ell(-\Omega_1\Gamma_2+\Omega_2\Gamma_1)(\Omega_1^2+\Omega_2^2)\,.
\end{aligned}
$$

Here, the second equation comes from the third equation of (2.12), the third equation is coming from ($\Gamma_1\times$ (eqn 1)+$\Gamma_2\times$ (eqn 2)) and the fourth is from ($\Omega_1\times$ (eqn 1)+$\Omega_2\times$ (eqn 2)) in the previous system (2.12).

Thus, the system is reduced to a system between the invariant variables (2.13) and the angle can be integrated once the system of invariant variables are integrated. Then, the conservation law of the rotational symmetry will be associated to the constant of integration of the derivative of angle, θ, and its symmetry action can be associated to the translation of angle if an initial condition is given.

We introduce the new invariant variables:

$$J_1 := \Gamma_3\,,\ J_2 := \Omega_3\,,\ J_3 = \Omega_1\Gamma_1 + \Omega_2\Gamma_2\,,\ J_4 := \Omega_1^2 + \Omega_2^2\,.$$

Following the analysis of [Olv93], we can divide the previous system by $d\theta/dt$ and the angle can replace the time. Then we get a same system with respect to θ,

$$\frac{d\theta}{dt} = \frac{d}{dt}\left(\tan^{-1}(\frac{\Gamma_2}{\Gamma_1})\right) = \frac{J_1^2J_2 + J_1J_3 - J_2}{1-J_1^2}$$

and

$$
\begin{aligned}
&\frac{dJ_1}{d\theta} = \left(\sqrt{J_4(1-J_1^2)-J_3^2}\right)\frac{1-J_1^2}{J_1^2J_2+J_1J_3-J_2}\,,\\
&(I_3+mr^2-mr^2J_1^2)\frac{dJ_2}{d\theta} - mr^2(J_1+\ell/r)\frac{dJ_3}{d\theta}\\
&= mr^2J_1J_2\left(\sqrt{J_4(1-J_1^2)-J_3^2}\right)\frac{1-J_1^2}{J_1^2J_2+J_1J_3-J_2}\,,\\
&- mr^2(1-J_1^2)(J_1+\ell/r)\frac{dJ_2}{d\theta} + (I_1+m\ell^2+mr^2J_1^2+2mr\ell J_1)\frac{dJ_3}{d\theta}\\
&= -J_2(I_3+mr^2J_1^2+mr\ell J_1)\left(\sqrt{J_4(1-J_1^2)-J_3^2}\right)\frac{1-J_1^2}{J_1^2J_2+J_1J_3-J_2}\,,\\
&(I_1+m(r^2+\ell^2)+2mr\ell J_1)\frac{dJ_4}{d\theta} - 2mr^2J_3\left(\frac{dJ_3}{d\theta}+(J_1+\ell/r)\frac{dJ_2}{d\theta}\right)\\
&= 2mr(rJ_2J_3-\ell J_4)\left(\sqrt{J_4(1-J_1^2)-J_3^2}\right)\frac{1-J_1^2}{J_1^2J_2+J_1J_3-J_2}\,.
\end{aligned}
$$

This reduced system of invariant variables, $J_1, \ldots, J_4$, is again invariant under the new scaling symmetry ation,

$$
\Omega \to e^{\epsilon}\Omega\,,\ \Gamma\to\Gamma \ \Rightarrow J_1\to J_1\,,\ (J_2,J_3)\to e^{\epsilon}(J_2,J_3)\,,\ J_4\to e^{2\epsilon}J_4\,.
$$

We choose the following variables as a explicitly straightened variable, τ, and invariant variables, K_i.

$$
\begin{aligned}
&\tau := \log(\Omega_3) = \log(J_2)\,,\ K_1 := \Gamma_3 = J_1\,,\\
&K_2 := \frac{\Omega_1\Gamma_1+\Omega_2\Gamma_2}{\Omega_3} = \frac{J_3}{J_2}\,,\ K_3 = \frac{\Omega_1^2+\Omega_2^2}{\Omega_3^2} = \frac{J_4}{J_2^2}\,.
\end{aligned}
$$

Then some of basic derivatives become

$$\begin{aligned}
\frac{d\tau}{d\theta} &= \frac{d(\log J_2)}{d\theta} = \frac{1}{J_2}\frac{dJ_2}{d\theta} \\
&= \frac{mr^2(I_1J_1 - I_3(J_1 + \ell/r))}{I_1I_3 + I_3m(\ell + rJ_1)^2 + I_1mr^2(1 - J_1^2)} \left(\sqrt{J_4(1 - J_1^2) - J_3^2}\right) \frac{1 - J_1^2}{J_1^2J_2 + J_1J_3 - J_2}\,, \\
\frac{dJ_2}{d\tau} &= J_2\,, \\
\frac{dJ_3}{d\tau} &= \frac{d}{d\tau}(K_2J_2) = (\frac{dK_2}{d\tau}J_2 + K_2\frac{dJ_2}{d\tau}) = J_2(K_2 + \frac{dK_2}{d\tau})\,, \\
\frac{dJ_4}{d\tau} &= \frac{d}{d\tau}(K_3J_2^2) = J_2^2(2K_3 + \frac{dK_3}{d\tau})\,.
\end{aligned}$$

And we get the next reduced system by dividing the previous system in J_i's by $d\tau/d\theta$. The previous system will transform to the following system of equations.

$$\begin{aligned}
&\frac{dK_1}{d\tau} = \frac{I_1I_3 + I_3m(\ell + rJ_1)^2 + I_1mr^2(1 - J_1^2)}{mr^2(I_1J_1 - I_3(J_1 + \ell/r))} \\
&= \frac{I_1I_3 + I_3m(\ell + rK_1)^2 + I_1mr^2(1 - K_1^2)}{mr^2(I_1J_1 - I_3(K_1 + \ell/r))}\,, \\
&I_3 + mr^2(1 - K_1^2) - mr^2(K_1 + \ell/r)(K_2 + \frac{dK_2}{d\tau}) \\
&= \frac{K_1(I_1I_3 + I_3m(\ell + rK_1)^2 + I_1mr^2(1 - K_1^2))}{(I_1K_1 - I_3(K_1 + \ell/r))}\,, \\
&- mr^2(1 - K_1^2)(K_1 + \ell/r) + (I_1 + m(\ell + rK_1)^2)(K_2 + \frac{dK_2}{d\tau}) \\
&= -(I_3 + mr^2K_1^2 + mr\ell K_1)\frac{(I_1I_3 + I_3m(\ell + rK_1)^2 + I_1mr^2(1 - K_1^2))}{mr^2(I_1K_1 - I_3(K_1 + \ell/r))} \\
&(I_1 + m(r^2 + \ell^2) + 2mr\ell K_1)(2K_3 + \frac{dK_3}{d\tau}) - 2mr^2K_2(K_2 + \frac{dK_2}{d\tau} + K_1 + \ell/r) \\
&= 2mr(rK_2 - \ell K_3)\frac{(I_1I_3 + I_3m(\ell + rK_1)^2 + I_1mr^2(1 - K_1^2))}{mr^2(I_1K_1 - I_3(K_1 + \ell/r))}
\end{aligned}$$

where the four equations in three unknowns, $K_{1,2,3}$ are a direct conversion from the previous system of variables J_i. The second and third equations of this system are reduced to the same equation and we get the reduced system of equations in

K_i's.

$$\begin{aligned}
&\frac{dK_1}{d\tau} = \frac{I_1 I_3 + I_3 m(\ell + rK_1)^2 + I_1 mr^2(1 - K_1^2)}{mr(rI_1K_1 - I_3(rK_1 + \ell))}\,,\\
&K_2 + \frac{dK_2}{d\tau} = \frac{-I_3(I_3 + m(r^2 + r\ell K_1)}{mr(rI_1K_1 - I_3(rK_1 + \ell))}\,,\\
&\frac{2(I_1 - I_3)[rI_1K_1 + mrK_1(r^2 + \ell^2) + mr^2\ell(1 + K_1^2)]}{rI_1K_1 - I_3(rK_1 + \ell)}K_3\\
&+ (I_1 + m(r^2 + \ell^2) + 2mr\ell K_1)\frac{dK_3}{d\tau}\\
&= \frac{2rK_2(I_1 - I_3)(I_3 + mr^2 + mr\ell K_1)}{rI_1K_1 - I_3(rK_1 + \ell)}\,.
\end{aligned}$$

This final system gives the Routh integral from the integration of the first equation of the system and the Jellett integral from the integration of the second equation of the system as

$$\begin{aligned}
R &= \Omega_3\sqrt{I_1I_3 + mr^2(I_1\Gamma_1^2 + I_1\Gamma_2^2 + I_3(\Gamma_3 + \ell/r)^2}\\
&= e^\tau\sqrt{I_1I_3 + I_3m(\ell + rK_1)^2 + I_1mr^2(1 - K_1^2)}\,,\\
J &= r(I_1\Omega_1\Gamma_1 + I_1\Omega_2\Gamma_2 + I_3\Omega_3(\Gamma_3 + \ell/r)) = e^\tau(rI_1K_2 + I_3(rK_1 + \ell))\,.
\end{aligned}$$

And the integration of the third equation from the system gives the conservation law of the total energy,

$$\begin{aligned}
H &= < I\Omega + s \times (m\Omega \times s), \Omega >\\
&= (I_1 + m|s|^2)(\Omega_1^2 + \Omega_2^2) + (I_3 + m|s|^2)\Omega_3^2 - m(r(\Omega_1\Gamma_1 + \Omega_2\Gamma_2) + \Omega_3(r\Gamma_3 + \ell))^2\\
&= e^{2\tau}[(I_1 + m(r^2 + \ell^2) + 2mr\ell K_1)K_3 + (I_3 + m(r^2 + \ell^2) + 2mr\ell K_1)\\
&- m(rK_2 + rK_1 + \ell)^2]
\end{aligned}$$

Hence the conservation laws of R, J and H come as the constants of integration from the above system. These conservation laws are left as the last three equations

after the original system has been reduced by the symmetry actions of the rotation and the scaling action.

The solution of this nonlinear system of differential equations for the rolling ball is completed as follows

$$
\begin{aligned}
& K_1 = K_1(\tau, R)\,,\ K_2 = K_2(\tau, K_1, J) = K_2(\tau, R, J)\,,\ K_3 = K_3(\tau, R, J, H)\,, \\
& \frac{d\theta}{d\tau} = f_1(K_1, K_2, K_3) \ \Rightarrow\ \theta = \int_{\tau_0}^{\tau} f_1(K_1, K_2, K_3)d\tau + \theta_0 = F_1(\tau, R, J, H) + \theta_0\,, \\
& \frac{dt}{d\tau} = \frac{dt}{d\theta}\frac{d\theta}{d\tau} = f_2(\tau, K_1, K_2, K_3) \ \Rightarrow\ t = \int_{\tau_0}^{\tau} f_2(\tau, K_1, K_2, K_3)d\tau + t_0 \\
& \quad = F_2(\tau, R, J, H) + t_0\,.
\end{aligned}
$$

The process of back-solving involves only direct integrations. And $(R, J, H, \tau_0, \theta_0, t_0)$, these 6 constants and a certain value of τ will determine the current state of variables. Actually K_i, θ and t as functions of τ are less number of dependent variables than the original system had and additional equation for determining the original system come as the conservation of the geometric condition, $\Gamma_1^2 + \Gamma_2^2 + \Gamma_3^3 = 1$.

Now we still want some answers for the puzzle of associating the conservation laws of R, J and H with corresponding symmetries. The internal symmetry of cylindrical mass distribution enables the rotational symmetry action on the system of equations. Without this rotational symmetry, the reduction by rotational invariance would not work. Then the only possible reduction would come from the scaling symmetry.

Hence in the free rolling motion of the imbalanced and non-symmetric ball, it seems be lacking the Lie symmetries to reduce the system into completely integrable

system. However there has been found another conservation law in [BM02b].

$$B =< I\Omega + s \times (m\Omega \times s), I\Omega - m < \Omega, s > s > \ .$$

Thus the scaling symmetry seems to be connected to the conservation law of B since this conserved quantity survives when the cylindrical symmetry breaks [BM02b]. Thus in the free rolling motion of Chaplygin's ball, the H and B are two most general conservation laws, but it is still not sufficient number of conservation laws to provide a complete integrability of the system. However, the understanding of connecting the rotational symmetry to the conservation laws of R and J is still very obscure and remains as unanswered question in this approach.

2.3.2 Extension to cylindrically symmetric rolling ball under gravity

Interestingly the rotational symmetry is still preserved under the extension to include the gravity field that is normal to the plane of rolling if the mass distribution of the rolling ball is cylindrically symmetric. The extended system of equations can be explicitly given as follows.

$$
\begin{aligned}
&(I_1 + m(r^2+\ell^2) + 2mr\ell\Gamma_3)\dot{\Omega}_1 - mr^2(\dot{\Omega}_1\Gamma_1 + \dot{\Omega}_2\Gamma_2 + \dot{\Omega}_3(\Gamma_3 + \ell/r))\Gamma_1 \\
&= -mr\ell(-\Omega_1\Gamma_2 + \Omega_2\Gamma_1)\Omega_1 + mr\ell(\Omega_1\Gamma_1 + \Omega_2\Gamma_2 + \Omega_3(\Gamma_3 + \ell/r))\Omega_2 \\
&+ m\gamma\ell\Gamma_2 + (I_1 - I_3)\Omega_2\Omega_3\,, \\
&(I_1 + m(r^2+\ell^2) + 2mr\ell\Gamma_3)\dot{\Omega}_2 - mr^2(\dot{\Omega}_1\Gamma_1 + \dot{\Omega}_2\Gamma_2 + \dot{\Omega}_3(\Gamma_3 + \ell/r))\Gamma_2 \\
&= -mr\ell(-\Omega_1\Gamma_2 + \Omega_2\Gamma_1)\Omega_2 - m\ell(\Omega_1\Gamma_1 + \Omega_2\Gamma_2 + \Omega_3(\Gamma_3 + \ell/r))\Omega_1 \\
&- m\gamma\ell\Gamma_1 - (I_1 - I_3)\Omega_1\Omega_3\,, \\
&(I_3 + m(r^2+\ell^2) + 2mr\ell\Gamma_3)\dot{\Omega}_3 - mr^2(\dot{\Omega}_1\Gamma_1 + \dot{\Omega}_2\Gamma_2 + \dot{\Omega}_3(\Gamma_3 + \ell/r))(\Gamma_3 + \ell/r) \\
&= -mr\ell(-\Omega_1\Gamma_2 + \Omega_2\Gamma_1)\Omega_3\,, \\
&\dot{\Gamma}_1 = -\Omega_2\Gamma_3 + \Omega_3\Gamma_2\,, \\
&\dot{\Gamma}_2 = -\Omega_3\Gamma_1 + \Omega_1\Gamma_3\,, \\
&\dot{\Gamma}_3 = -\Omega_1\Gamma_2 + \Omega_2\Gamma_1
\end{aligned}
$$

where γ is the acceleration of gravity.

The scaling symmetry would be still valid if additional scaling action on the acceleration of gravity is assumed as $\gamma \to e^{2\epsilon}\gamma$. The same application of the rotational symmetry and the scaling symmetry will integrate the system.

In this system of cylindrically symmetric rolling ball under gravity, the conservation of B is no longer valid, but the conservation of H, R and J will be still effective. With the addition of geometric condition $|\Gamma|^2 = 1$, these conservation laws will make the system still integrable as proved by Chaplygin [Cha02]

2.4 Comparison between the Noether's theorem and the symmetry reduction

Using Noether theorem and symmetry reduction by Lie symmetries, we wanted to see how we get the conservation laws from symmetries and how to connect

them. Now which connection between Noether symmetry and Lie symmetry is easier to find? And which one is giving more understandable connection to the corresponding conservation law? Noether symmetry of the action integral or Lie symmetry of the system of differential equations?

There seems not be the general answer to this question. However, in the problem of Chaplygin's rolling ball the Lie symmetry looks like being more straightforward application of symmetries that lead to their corresponding conservation laws. The symmetry vectors for Noether symmetries, η, are not physically nor mathematically clear about how to find them. And at this point, their meaning of Noether symmetry vectors are not clear yet.

The weakness of Lie symmetry is that a Lie symmetry cannot be directly associated to a conservation law because the symmetry is used to reduce the degree of the system of equations by one and still requires the integration of the reduced system to get a conserved quantity to be associated to the Lie symmetry action. However, the Noether symmetry has direct association to a conservation law if a Noether symmetry exists for the Lagrangian system.

Hence there are their own advantages on both sides of approaches to the symmetries of the system. Further studies could clarify the picture on interpreting the related symmetry actions and getting the two approaches to be related each other.

Chapter 3

AN ENSEMBLE OF ROLLING WATER MOLECULES AS A MODEL FOR MOLECULAR MONOLAYER

(This paper has been accepted in the journal Physical Review Letters.)

Rolling motions have many applications in our daily life, for example, many machines with rolling parts, like bicycles or automobiles. In this chapter, we tried to find applications of the rolling dynamics in an experimental setting of rolling bodies in molecular scale. The rolling constraint imposes very interesting restriction of motion due to its non-integrability. Hence we found the dynamics of a system under such nonholonomic constraint would show interesting aspect of physics. The study is focused on how the nonholonomic rolling constraint affects on the basic statistical quantities in the system of many interacting particles.

3.1 Introduction

Molecular monolayers are playing an ever increasing role in technology as they allow manipulation of contact properties of materials in a precise and controlled manner. There have been considerable effort in analyzing the structure of molecular monolayers; in particular, self-assembled polymeric monolayers [Ulm96, MKL02]

and water monolayers with TIP5P model [ZM03]. Previous theoretical work on molecular monolayers has concentrated on either static studies of monolayer structures [CMF$^+$09, Ulm96] or molecular dynamics simulations where each molecule is moving under the forces and torques from surrounding molecules and the substrate [MKL02, Kum10, ZM03, KYX$^+$06]. The direct molecular simulations employed in these papers were quite successful in explaining various properties of liquid water, *e.g* formation of contact angle [MKL02] or anomalous properties for nano-confined water [KYX$^+$06, Kum10]. In the latter papers, the confinement of water molecules to a very thin layer was achieved by physically constraining the bulk of water to a very narrow (nm) layer by the rigid surface on both sides. On the other hand, experimental data demonstrate the presence of a water monolayer on a Si surface under normal conditions, which is due to the strong bond between the water molecules and the substrate [MXSS98, CMF$^+$09]. Such a bond is difficult to account for in the atomistic molecular simulations of TIP5P type. On the other hand, one would like to keep the relative simplicity of atomistic models without introducing extra coupling bonds, the nature of which are not well understood.

The purpose of this study is to suggest a simple yet physical way of introducing a strong coupling bond between the monoloayer molecules and the substrate as a rolling constraint. We assume that the bonds between the substrate and the molecule are very short ranged and thus act on the part of the molecule in close contact with the substrate atoms. Physically, that leads to the fact that while the molecule itself is moving, its point of contact with the substrate is stationary. This invokes the analogy with a classical problem of rolling body on the surface with perfect friction, appearing when the bond molecule-substrate is infinitely strong at contact point, but decays rapidly away from substrate. In reality, if that bond is

large but finite, the motion will be a combination of sliding and rotating. However, the theory of sliding and rolling is not yet well developed [RDG94, BMZ05], and so in this paper we will restrict ourselves to the simplest possible realization when the friction is perfect. Thus, we consider the dynamics of a monolayer consisting of rolling molecules that are self-interacting by the long-range interactions (Lennard-Jones and electrostatic), while the influence of the boundary is limited to restricting the motion to the perfect rolling dynamics. While the rolling dynamics may seem too idealized, it has actually been observed in the context of functional nano-structures [SOZ$^+$06]. More complex models of molecule-substrate interaction are possible, resulting in the gravity-like component in the force acting on the ball, but such interactions will not be considered here.

The study of rolling motion of rigid bodies has a long history in the context of classical mechanics [Blo03, BMZ05, Gol01]. However, the study of collective motion of rolling particles has not been undertaken. The non-holonomic rolling constraint is a major obstacle in the way of constructing statistical mechanics for the rolling particle systems [Tar05, GL, Kut99, LL80]. This study is devoted to defining ordered and disordered states of the rolling particle systems (akin to solid and gas/liquid), and computing statistical physics concepts for such systems. We also show the way rolling affects propagation of phonons through a rolling particle lattice, which opens the way to experimentally confirm the molecular rolling motion.

3.2 Concepts in statistical mechanics

The statistical mechanics, or thermodynamics, are developed as microscopic equivalent of gas theory which was based on empirical observations and behavior of a gas in macroscopic terms. The basic theory of the thermodynamics redefined the

properties of a gas in mathematical and statistical concepts.

The theory is based on the assumption of ideal gas, which assumes the following postulates [Bla].

1. A gas consists of a collection of small particles traveling in straight-line motion and obeying Newton's Laws.

2. The molecules in a gas occupy no volume (that is, they are point masses).

3. Collisions between molecules are perfectly elastic (that is, no energy is gained or lost during the collision).

4. There are no attractive or repulsive forces between the molecules.

5. The average kinetic energy of a molecule is 3kT/2. (T is the absolute temperature and k is the Boltzmann constant.)

Under these assumptions of an ideal gas, the small non-interacting particles exchange velocities through many collisions and come to the state of thermodynamic equilibrium. Statistical properties of gas contained in finite volume can be determined.

Many macroscopic properties of a system can be defined as average quantities in the ensemble of the system. The ensemble of a thermodynamic system is the collection of all the possible microscopic states which share one or more macroscopic properties (e.g. the same total energy of the system). The system evolves in time visiting those states. For example, the members of the ensemble of same total energy can differ in their kinetic energies. Then still some macroscopic properties on different microscopic systems in the ensemble could be the same as they are

defined as averaged quantities and such macroscopic observables such as temperature and pressure can be calculated by averaging over the whole ensemble [Tuc]. A macroscopic property, A, of the system can be calculated as the average of a microscopic function a,

$$A_{macro} = \frac{1}{N} \sum_{\lambda=1}^{N} a_{\lambda,micro}$$

where N is the total number of members in the ensemble and a_λ is the value of a microscopic function a in the λ-th member. In other words, a thermodynamic property of a system can be calculated as an ensemble average of the corresponding microscopic function.

Now the statistical distribution can be defined on the ensemble. For example, on the ensemble of the same total energy, the members of the ensemble may have different kinetic energies. The ensemble will have all the members of every possible kinetic energies, E_i. Then the number of members in the energy state of E_i can be associated as the function of energy states in the ensemble and this function can define a statistical distribution in the ensemble.

Since the physical system of the ensemble evolves in time, some members of the ensemble can be visited by a trajectory of time-evolving system from on initial state and some other members may need the system to evolve from a different initial state. However the usual hypothesis is the *ergodic hypothesis*.

Definition 3.2.1 (Ergodic hypothesis)**.** *An* ergodic *system is a system which, given an infinite amount of time, will visit all possible microscopic states available to it.*

According to the ergodic hypothesis, if a system is ergodic, then the ensemble average of a property will be equal to the time average of the property in an ergodic

trajectory.

For an ideal gas, the statistical distribution function becomes the Maxwell-Boltzmann distribution for a canonical ensemble of the system.

Definition 3.2.2 (Boltzmann distribution)**.** *The proportion of members in the ensemble occupying a set of states i with energy, E_i, is*

$$\frac{N_i}{N} = \frac{g_i \exp(E_i/kT)}{\sum g_i \exp(E_i/kT)} \tag{3.1}$$

where N_i and N are the number of members in the state i and the total number in the ensemble and g_i is the degeneracy of the state i. k is the Boltzmann constant and T is the temperature of the system.

If there is no degeneracy ($g_i = 1$), then the distribution simplifies to

$$\frac{N_i}{N} = \frac{\exp(E_i/kT)}{\sum \exp(E_i/kT)}\,.$$

Thus the distribution function of the translational velocity of point masses in one direction becomes

$$f(v_x) = \sqrt{\frac{m}{2\pi kT}} \exp(\frac{-mv_x^2}{2kT}) \tag{3.2}$$

The temperature of an ideal gas system is defined as a macroscopic property.

Definition 3.2.3 (Temperature)**.** *The temperature of an ideal gas with Boltzmann distribution (3.2) is the average of the (translational) kinetic energy of the system.*

$$\frac{3}{2}kT = < \frac{1}{2}mv^2 > = \sum_{i=1}^{3} < \frac{1}{2}mv_i^2 >$$

where the average of each directional kinetic energy becomes $kT/2$.

Definition 3.2.4 (Equipartition of energy)**.** *In thermal equilibrium, the energy of a system is shared equally among all of its various forms.*

According to the equipartition of energy, the translational kinetic energy of an ideal gas is all same as $kT/2$ in any directional motion in 3D and the total energy becomes $3kT/2$. If the molecules of the system has rotational components in its kinetic energy, then each rotational component of kinetic energy will share the same energy as any one of translational component of the energy.
Hence, the temperature of an ideal is the ensemble average of the kinetic energy of the system and it also determines the Boltzmann distribution of the system. Moreover, the temperature can be calculated from the distribution of the velocity in one direction if the system follows such a Boltzmann distribution (3.1).

$$\log(\frac{N_i}{N}) = \frac{1}{kT}E_i - \log(\sum \exp(E_i/kT))$$

and $1/kT$ can be computed as the slope of the linear graph of the kinetic energy and $\log(N_1/N)$ or the kT/m can be found as the variance of the normal distribution of the one component of velocity in (3.2). Since the directions are indistinguishable in the motion of point masses of an ideal gas, the choice of any velocity component doesn't affect on the distribution function and on computation of temperature as the variance of the distribution.

In our study of the system of many rolling particles, we have tried to extend the concepts of statistical mechanics into the rolling-constrained system.

3.3 Setup of the dynamics

The rolling particles are simulated as identical spherical rigid bodies of radius r all having the same mass m and the moments of inertia tensors. The center of mass is assumed to be at a position different from the geometric center, as illustrated

on Fig. 3.1. The notation used in this paper is as follows: $\mathbf{\Gamma}_i$ is the unit vector pointing to the geometric center (GC), $\mathbf{\Omega}$ is the angular velocity *in the ball's coordinate frame* and $\mathbf{s}_i$ is the vector pointing to the center of mass (CM). The

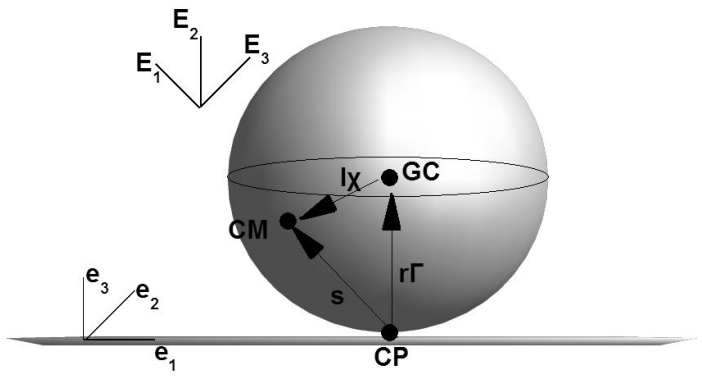

Figure 3.1: Schematic and definitions of an offset rolling ball dynamics.

equations of motion for an individual ball come from the well-known Chaplygin's equations [BMZ05, BM02a]. Under certain symmetry conditions, Chaplygin's ball is completely integrable and has three integrals of motion: one is total energy that is the easily understandable physical quantity. The other two constants of motion are Routh and Jellet integrals that are harder to explain in terms of elementary physics [GN00]. The equations of motion for the i-th ball are as follows:

$$\left(\frac{d}{dt} + \mathbf{\Omega}^i\times\right)\left(I^i\mathbf{\Omega}^i + m\mathbf{s}^i \times (\mathbf{\Omega}^i \times \mathbf{s}^i)\right) - m^i\dot{\mathbf{s}}^i \times (\mathbf{\Omega}^i \times \mathbf{s}^i) = s^i \times \mathbf{F}^i + \mathbf{T}^i \tag{3.3}$$

$$\frac{d\mathbf{\Gamma}^i}{dt} = -\mathbf{\Omega}^i \times \mathbf{\Gamma}^i\,. \tag{3.4}$$

Here, I^i are the eigenvalues of the tensor of inertia and $\mathbf{F}^i$ and $\mathbf{T}^i$ are the total force and torque acting on the ith particle. These forces and torques include the inter-particle interactions. The rolling constraint for velocity of the center of mass $\mathbf{V}^i$,

written as $\mathbf{V}^i = \mathbf{\Omega}^i \times \mathbf{s}^i$ cannot be reduced to an equation between configuration variables only, and is thus non-holonomic [Blo03]. The Hamiltonian approach for the ensemble of rolling ball cannot be defined, and thus it is impossible to construct a meaningful approach for this system by simply extending the classical statistical physics to this case. Note that neither linear nor angular momenta are conserved, neither for individual particles nor for the whole system. The total energy of the system, however, is conserved.

The inter-molecular interactions causes the interchange of linear and angular momentum as well as energy between particles. In the simulation of rolling water molecules, the Lennard-Jones (LJ) potential V_{LJ} and the dipole potential V_d are considered. The dipole $\mathbf{p}_i$ is positioned at the center of mass on each spherical particle. The interactions we consider are defined as follows:

$$V_{LJ} = 4\epsilon \sum_{i \neq j} \left(\frac{\sigma^{12}}{r_{ij}^{12}} - \frac{\sigma^6}{r_{ij}^6} \right), \tag{3.5}$$

$$V_d = \frac{1}{8\pi\epsilon} \sum_{i \neq j} \mathbf{p}_i \cdot \left(\frac{3(\mathbf{p}_j \cdot \hat{r_{ij}})\hat{r_{ij}} - \mathbf{p}_j}{r_{ij}^3} \right). \tag{3.6}$$

To be concrete, in the computations of collective dynamics for rolling particles, we use the parameters and interactions relevant to water molecule monolayers by choosing the mass $m = 2.991 \cdot 10^{-23}$ g, moments of inertia $(I_1, I_2, I_3) = (0.2076, 0.1108, 0.3184) \cdot 10^{-39}$ g·cm^2, radius $r = 1$ Å, displacement of center of mass from the geometric center $\ell = 0.068$Å, dipole moment $6.17 \cdot 10^{-30}$ (C $\cdot$ m), LJ radius $\sigma = 3.165$ Å and energy $\epsilon = 0.650$kJ/mol. These values correspond to the parameters of a water molecule [BPvGH81]. For convenience, we choose the angular velocity scale $\tilde{\omega} = 10^{13}$rad/s. The rolling constraint then introduces the scaling of velocity to be $\tilde{v} = r\tilde{\omega} = 10$cm/s. Given a different set of parameters, the details of our computations will be different, but the methods and results outlined

here hold for other molecules as well. For the set of parameters considered here, neither Routh nor Jellet integrals for each ball are conserved.

3.4 Stationary states: a crystalline lattice

The existence of stationary states for the system of rolling particles depends on the presence and orientation of the dipole moment. Suppose for now that the dipole moment is absent, and the only interaction between the molecules is Lennard-Jones. Suppose also for the moment that the particles are not moving, and are aligned so both geometric center and center of mass are along $\mathbf{\Gamma}$, the unit vector pointing upward from the contact point. It is easy to see then that there is an equilibrium configuration so that the centers of mass are arranged at a distance close to σ, the equilibrium distance of LJ potential. For the case of two and three particles, there is an equilibrium configuration where the particles are arranged at exactly the distance σ from each other.

Let us suppose now that these particles are spun with angular velocity $\mathbf{\Omega}_i = (0, 0, \Omega_i)$ that is pointing upwards. In the absence of nonlocal interaction this will be a neutrally stable state for each particle, although friction forces may destabilize such equilibria, similar to familiar phenomenon of the tippe top [BRMR08]. Because LJ forces are exactly at balance, independent of the values of Ω_i, this will be an equilibrium state. In the presence of the dipole moment, finite lattices cease to be equilibrium configurations. However, if the dipole moment points exactly along the line from the geometric center to the center of mass (which is the case for the particles considered here), an infinite regular lattice, possessing high symmetry (like a triangular or square lattice) will still be an equilibrium state. The dipole moments can either be arranged in the same directions or be alternating. However,

the states with the dipole moments all pointing in one direction are unstable both linearly and nonlinearly. Thus, in what follows we concentrate on the states with the alternating dipole moments as shown on Figure 3.2.

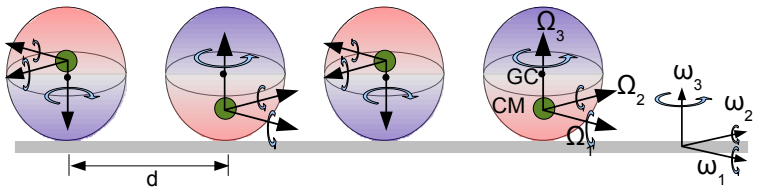

Figure 3.2: Schematic representation of stationary states.

A question about the stability of these states immediately arises. While a detailed investigation of the stability is a complex issue beyond the scope of this discussion, a simple physical explanation can be made showing that these states are linearly unstable. Suppose for simplicity that all rotation rates are the same, $\mathbf{\Omega}_i = \mathbf{\Omega}_0$. A small perturbation in the spinning stationary state will result to a precession of each particle, which according to the rolling constraint will happen at the same rate as the rotation frequency. The distance between particles will also change with the same frequency, and through the LJ interaction (3.5) both particles will experience parametric resonance. Similar argument applies to different rotation rates, and more particles in a lattice. Thus, all lattice states are linearly unstable. However, these states are *nonlinearly stable* at least for some of the configurations and initial conditions we have investigated, corresponding to low initial energies. In Fig. 3.3, left, we show the positions of the centers of 81 rolling balls situated in a rectangular lattice, over a long simulation time. While each particle remains close to its equilibrium position, the individual trajectories (blow-up on the same Figure) are chaotic and are strongly reminiscent of thermal vibrations in lattices.

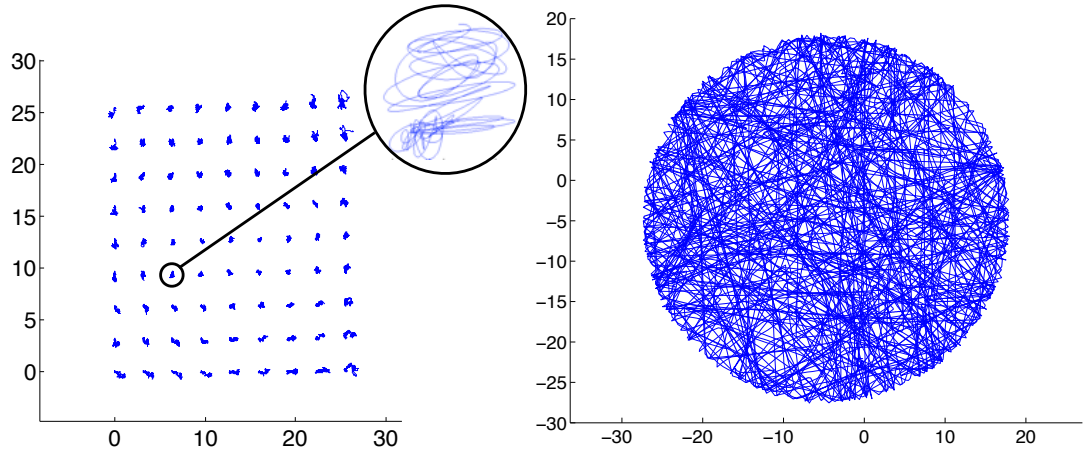

Figure 3.3: Left: trajectory of the center of rolling particles in lattice model, with the blow-up showing the trajectory of an individual particle. The finite lattice is not an exact stationary state, so the vibrations are most apparent at the edges. Right: trajectories of a gas state in a circular container.

3.5 Lattice dispersion relation

In order to suggest a possible experimental verification of rolling motion, we suggest measuring the propagation of disturbances through the lattice. The derivation of dispersion relation for a lattice of spinning particles in general case is difficult, as it involves linearization about oscillating base states. If the equilibrium base state is a spinning state, then the linearized system involves time-periodic coefficients and it becomes a Floquet system. Here we consider an even simpler problem. We present the analysis of the rolling and rocking lattice with all the particles being stationary in the base state, *i.e.* $\Omega_i = 0$ in body frame or $\omega_i = 0$ in spatial frame. The body and spatial frames coincide initially. Assuming an infinite square lattice of rolling and rocking ball-shaped particles, we have the equations of motion for the i-th particle in spatial frame as,

$$\left(\frac{d}{dt}\right)(J^i\omega^i) + m\sigma^i \times \left(\left(\frac{d}{dt}\right)(\omega^i \times \sigma^i)\right) = \sigma^i \times F^i\,. \tag{3.7}$$

The system is perturbed from the stationary equilibrium state and the displacement of a particle from its equilibrium position is $D_{(i,j)}$ for the CM of the particle at the lattice index position of (i,j). Considering the small deviation is in the order of ϵ, the rolling condition in the perturbed motion becomes

$$\dot{D}_{(i,j)} = (0,0,r+\ell)^T \times \omega_{(i,j)}$$

where $D_{(i,j)}$ and $\omega_{(i,j)}$ are all in the order of ϵ. Componentwise, we get

$$\omega_{(i,j),x} = -\frac{\dot{D}_{(i,j),y}}{(r+\ell)}\,,\ \omega_{(i,j),y} = \frac{\dot{D}_{(i,j),x}}{(r+\ell)} \text{ and } \dot{D}_{(i,j),z} = 0\,.$$

Now, the force acting on the (i,j)-th particle is considered as the sum of the spring forces (linearization of LJ forces) from the 8 nearest-neighboring particles. Simply, we assumed the spring constants are all the same for all the 8 spring forces. We get the following vector sum of forces in the order of $O(\epsilon)$.

$$\begin{aligned}
F_{(i,j)} &= K < D_{(i+1,j)} - D_{(i,j)}, (1,0,0)^T > (1,0,0)^T \\
&+ K < D_{(i+1,j+1)} - D_{(i,j)}, (1,1,0)^T/\sqrt{2} > (1,1,0)^T/\sqrt{2} \\
&+ K < D_{(i,j+1)} - D_{(i,j)}, (0,1,0)^T > (0,1,0)^T \\
&+ K < D_{(i-1,j+1)} - D_{(i,j)}, (-1,1,0)^T/\sqrt{2} > (-1,1,0)^T/\sqrt{2} \\
&+ K < D_{(i-1,j)} - D_{(i,j)}, (-1,0,0)^T > (-1,0,0)^T \\
&+ K < D_{(i-1,j-1)} - D_{(i,j)}, (-1,-1,0)^T/\sqrt{2} > (-1,-1,0)^T/\sqrt{2} \\
&+ K < D_{(i,j-1)} - D_{(i,j)}, (0,-1,0)^T > (0,-1,0)^T \\
&+ K < D_{(i+1,j-1)} - D_{(i,j)}, (1,-1,0)^T/\sqrt{2} > (1,-1,0)^T/\sqrt{2}\,.
\end{aligned}$$

In addition, the zero order terms of some variables are

$$J_{(i,j),0} = (I_1, I_2, I_3)\,,$$
$$\sigma_{(i,j),0} = (0, 0, r+\ell)\,,$$
$$\omega_{(i,j),0} = (0, 0, 0)\,,$$
$$D_{(i,j),0} = (0, 0, 0)\,.$$

Finally, we get the linearized system as,

$$\begin{pmatrix} (I_1 + m(r+\ell)^2)(-\ddot{D}_{(i,j),y}/(r+\ell)) \\ (I_2 + m(r+\ell)^2)(\ddot{D}_{(i,j),x}/(r+\ell)) \\ 0 \end{pmatrix} = \begin{pmatrix} 0 \\ 0 \\ r+\ell \end{pmatrix} \times F_{(i,j)}\,. \tag{3.8}$$

Wave solutions for the perturbed rolling and rocking motion of this system can be tried in the form of

$$D_{(i,j)} = e^{-i(\omega t - k_x \cdot x - k_y \cdot y)}(D_x, D_y, 0)^T$$

where ω is the frequency of the wave and $k_x\,,\ k_y$ are the wave numbers. With this assumption of wave solution, the wave form of $D_{(i+1,j+1)}$ would become,

$$\begin{aligned} D_{(i+1,j+1)} &= e^{-i(\omega t - k_x \cdot a - k_y \cdot a)}(D_x, D_y, 0)^T \\ &= e^{i(k_x \cdot a + k_y \cdot a)} e^{-i(\omega t}(D_x, D_y, 0)^T \\ &= e^{i(k_x \cdot a + k_y \cdot a)} D_{(i,j)} \end{aligned}$$

where a is the length of the equilibrium lattice and the square lattice is assumed. We applied the wave form of solutions to equation (3.8) and obtained the system of equations for the directional vector (D_x, D_y) of the wave. Making the argument that the directional vector should exist, we make the determinant of the coefficient matrix become zero. Then we arrive to the following dispersion relation for the

propagation of disturbances of the form $e^{-i\omega t+ik_x x+ik_y y}$, (k_x, k_y) being the wave vector:

$$\begin{aligned}\Big\{\frac{m}{K}\big(1+\zeta_1\big)\omega^2-4+2\cos(k_x a)(1+\cos(k_y a))\Big\}\times\\ \Big\{\frac{m}{K}\big(1+\zeta_2\big)\omega^2-4+2\cos(k_y a)(1+\cos(k_x a))\Big\}\\ -4\sin^2(k_x a)\sin^2(k_y a)=0\,,\end{aligned}\tag{3.9}$$

where $\zeta_i = I_i/\big(m(r+\ell)^2\big)$, $K = d^2V_{LJ}/dr^2$ is the spring constant of the LJ potential and a is the periodicity of the square lattice . Note that (3.9) differs from the standard dispersion relation for a square lattice of springs only by the dimensionless coefficients ζ_i, incorporating the effects of rolling. For our values of parameters, $\zeta_i \simeq 0.1-0.2$. Thus, the rolling constraint affects the speed of sound by about 10-20%, which should be a measurable difference.

This dispersion relation (3.9) only makes sense within the periodicity domain $0 \leq (k_x, k_y) \leq 2\pi/a$. An example of two roots of $\omega(k)$ is given in Fig. 3.4. The frequency ω is always real.

The dispersion relation for a lattice consisting of non-rolling balls connected by LJ springs can be easily obtained from (3.9) by setting $I_1 = I_2 = 0$, $l = 0$. For the values of parameters chosen here, $\omega(k)$ for rolling and non-rolling balls differ by about 20%, which should be a noticeable and measurable difference.

3.6 Disordered states: statistical analysis

For large initial energies, the lattices become unstable, and in the absence of external boundaries the particles scatter to infinity, making the concepts of statistical physics meaningless. Thus, for large energies leading to gaseous states, we perform the simulations in a round potential well with sharp walls, forcing the particles to

remain within a circle. An example of such simulation with 16 particles is shown in Figure 3.3, right.

The first step towards considering this system as a statistical physics model is to investigate the distribution of linear and angular velocities. For an ideal gas in 3D, the Maxwell-Boltzmann distribution for velocities is

$$f_v(\mathbf{v}) = \left(\frac{m}{2\pi kT}\right)^{3/2} \exp\left(-\frac{m\mathbf{v}^2}{2kT}\right) , \tag{3.10}$$

and similar for the rotational degrees of freedom. The implicit assumption in (3.10) is that the distribution of velocities in each direction is normal with *the same* width that defines the temperature T of the system. However, in the system of rolling particles there is no reason for (3.10) to work: first, the rotational and translational components are coupled through the rolling constraint and second, even though the rolling motion is along the plane, each ball undergoes three-dimensional motion.

Figure 3.5 shows several examples of the distribution for several values of total energy of the system. On the left side of this Figure, we plot the distribution of ω_x, which is identical to the distribution of ω_y. These distributions are always very close to normal, which are shown with solid curves. The right side of this Figure shows distributions of ω_z for the same values of the energy, and it is apparent that this distribution is not normal. The distributions of v_x, v_y and v_z show the same tendencies. It is important to note, however, that the variances (in proper units) of normally distributed angular and linear velocities are *not* the same, and thus there is no straightforward definition of temperature for this system. We shall also note that due to the non-normal nature of the distribution in one of the components and the non-holonomic coupling between angular and linear velocities, the kinetic energy distribution does not follow Maxwell-Boltzmann law.

In addition, the kinetic energies of rotational and translational motion are not equal (even in a statistical sense), so the equipartition of energy in our system does not hold.

3.7 Temperature as scaled variance

Clearly, the rolling constraint prevents a straightforward statistical physics description of the rolling particle systems. Nevertheless, there is a surprising relation that connects the variances σ obtained from the angular (σ_ω) and linear (σ_v) velocities. Namely, we observed that for all values of in our numerical experiments, there is a surprising well-behaved linear relationship $\sigma_\omega = k\sigma_v$, with the coefficient $k \simeq 1.08$ depending only on the parameters on the system (geometry of the ball, center of mass position *etc*) but not on anything else. That relationship is valid for almost 6 orders of magnitude in lattice and gas states, as shown in Figure 3.6. We note that there is no *a priori* reason for such relationship to exist, but the surprising robustness of this law leads us to believe that it could be taken as one of the postulates in future development of statistical mechanics for non-holonomic gas.
Using this surprising relation we can define the temperature as the variance of either horizontal linear or angular velocity, or any linear combination of those. Since the temperature is defined up to a constant, all these definitions lead to the same results up to a scaling factor. Thus, on Figure 3.7, we plot the scaled variances vs total energy of the system. If we think of the variance W as being proportional to temperature, we observe that the total energy E is directly proportional to the temperature,which is reminiscent of ideal gas. Thus, in spite of complexities of the rolling systems, some aspects from the ideal gas remain. We shall note that since in simulations we use real balls interacting with LJ potential, a more

detailed simulation should show the effects of the finite size of the particles, but our simulations do not allow a reliable investigation of these effects.

Using the concept of temperature as scaled invariance, we can now define thermodynamically meaningful equations of state. On Figure 3.7, we plot the temperature as a function of the energy per particle. The equation of state for the lattice state (left panel of the Figure) ceases to exist for small negative energies as the lattice becomes unstable and ceases to exist. The exact nature of the destruction of lattice state is as yet unclear, but the divergence of the variance $\sigma^2 \sim (E_0 - E)^{-1}$ (shown in the insert) indicates the presence of a phase transition.

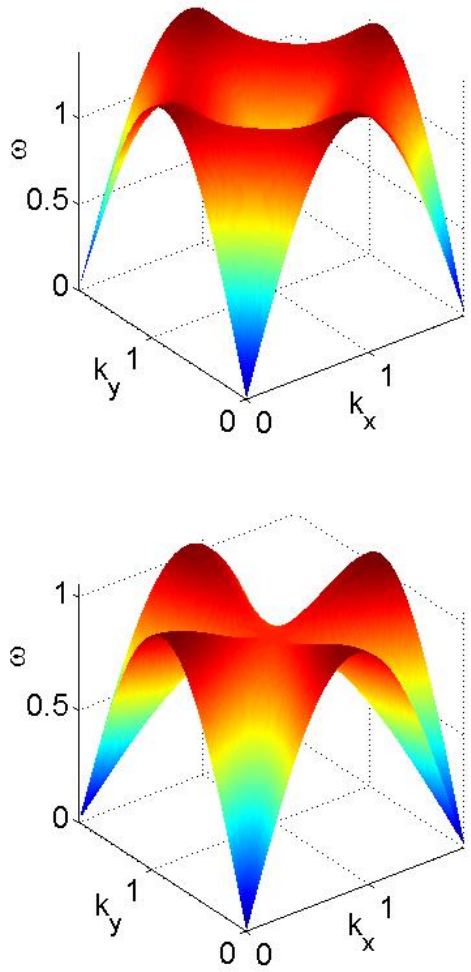

Figure 3.4: Dispersion relations given by two different roots of (3.9).

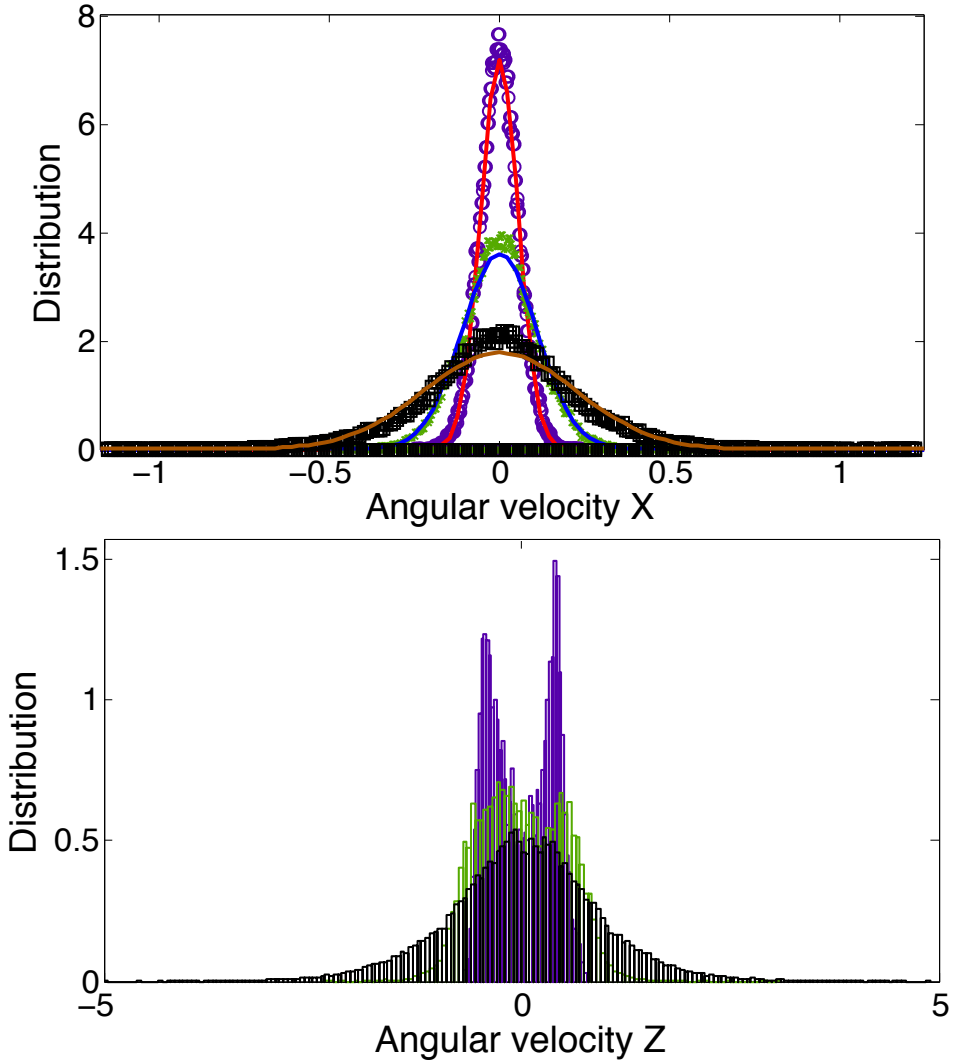

Figure 3.5: Distributions of ω_x (left) and ω_z (right) for different energies of the system. Solid curves represent fits to normal distributions.

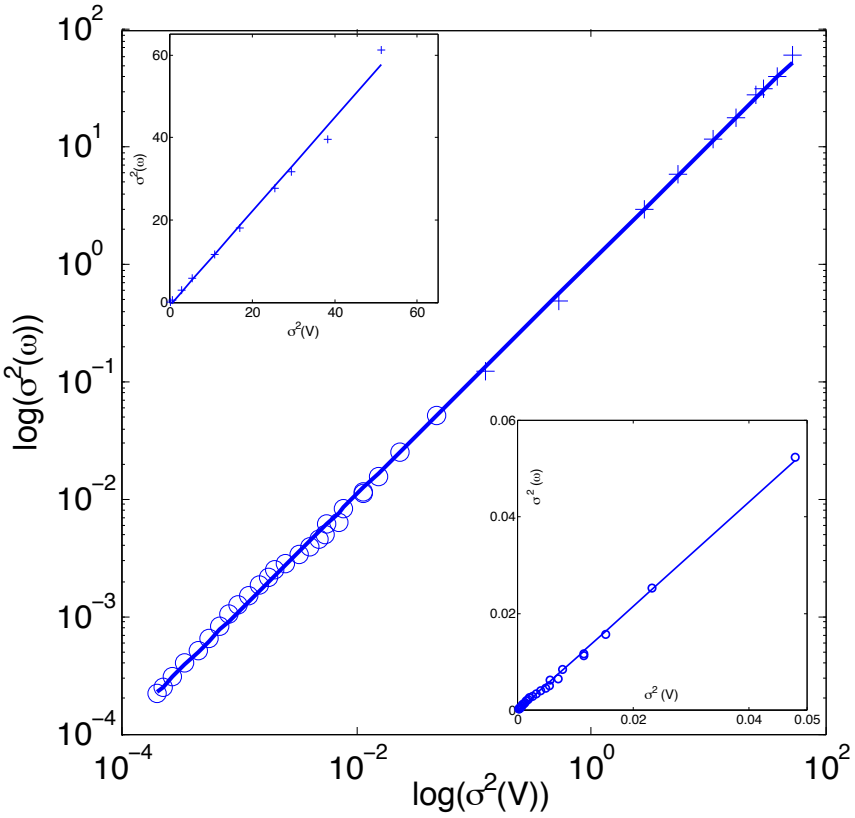

Figure 3.6: Linear relationship between variances σ_v and σ_ω for lattice states (circles) and gas states (lines). Common linear fit to both sets of data is also shown. The linear plots for each regime are shown as inserts.

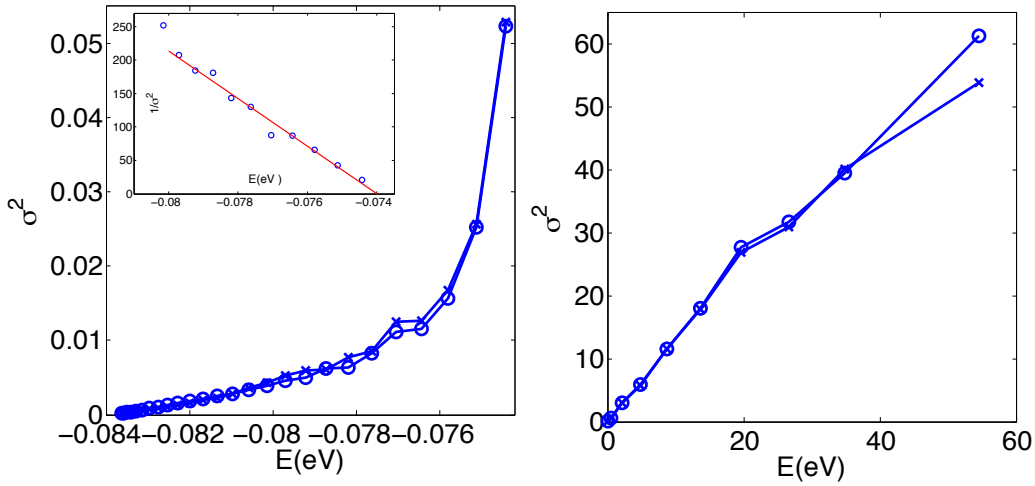

Figure 3.7: Variances vs energy in the lattice state (left) and gas state (right). Circles: $\sigma^2(\omega)$-distribution; crosses: $\sigma^2(v)$-distribution multiplied by $k = 1.08$. Left insert: $1/\sigma^2$ vs E.

Chapter 4

MANIPULATION OF SINGLE ATOMS USING AFM AS RESONANCE EFFECT

The previous chapters have discussed on the dynamics of system with rolling constraint. The detailed discussion on the evolution equations and the constraint of rolling condition is eventually applied to the simulation of the monolayer of water molecules which are idealized as perfectly rolling particles. Our attention to the nano-scale dynamics continues in this chapter. Recent experimental results of single atom manipulation motivated our study.

As electronic devices miniaturize, and the methods for small-scale manufacturing advance, the possibility of building useful structures out of individual atoms are becoming within our reach [TSZ04]. Recent development of dynamic force microscopy has demonstrated amazing capability of manipulating single atoms and building nano structures with single atoms [ES90, BMR97, SC04, OCY$^+$03, SCAM06, SPC$^+$08]. The techniques of manipulation of individual atoms have experienced an explosive development in the last two decades. Already, scanning tunneling microscopy (STM) has been used for atomic-scale imaging and manipulations [ES90, BMR97, SC04, Hla05]. However, STM operation is limited to electrically insulating surfaces. In contrast, an Atomic Force Microscope (AFM)

uses short range inter-atomic forces to directly probe and image material surfaces [SPA$^+$07].

Thus STMs and AFMs have been applied intensively as main tools for atom-manipulations on the semiconductor surfaces even though they were developed for their capability of the imaging power for atomic scale. Noticeably, recent experiments conducted in Osaka University have shown that the ultra high vacuum *non contacting* AFM (UHV-NCAFM) could realize very diverse manipulation of single atoms [OCY$^+$03, SCAM06, SPC$^+$08]. Such diverse controllability has immense potential importance of application in the fields of bio science and material science. Upon the observation of the experimental achievements, theoretical studies have followed to illuminate the mechanism of atomic manipulation using NCAFM [DvP05, Dv07, TWKS07, KPH09]. There are two points of view on the atomic control, quantum mechanical view and classical mechanical one. The solid silicon (Si) surface is formed as a regular lattice structure of Si atoms and many electrons are filling the space between those atoms. Thus the Si surface is a very complicated system consisting of many atomic particles and the manipulation of a single atom could be a very challenging process. Despite such challenges, amazingly diverse possibility of manipulation has been experimentally realized. Based on the experimental results, our study tries to illuminate the process under the view of mechanical resonance and shows that the dynamic interaction of atoms could result in such manipulation of single atoms. This part of our study was published in the journal of Physical Review Letters [KPH09].

4.1 Review: experiments on single atom manipulation

The experiments of atomic manipulations using NCAFM have been conducted in the Morita Laboratory in Osaka University, Japan. The results from those

experiments have been the subject of our study. Most experiments of manipulation using NCAFM have been conducted on the silicon surfaces since the silicon material is of high interest in the semiconductor industry. The solid silicon is formed as a very regular diamond lattice with four outermost electrons for an atom and they form covalent bonds between atoms. Even though the atoms form a regular lattice, they vibrate in their lattice position and the covalent bonds can break and form to make structural changes. The atomic resolution of image made by NCAFM has been so much improved by the lab and the NCAFM image could show the change in the atomic structure through the direct scanning of the silicon surface using the interaction between the atoms in Si surface and those in the AFM tip. The tip of NCAFM is itself a very sharp solid structure of silicon or other some other solid material. The approach of the AFM tip is delicately controlled by electronic feedback circuit so that the surface lattice is not damaged under the interaction with NCAFM tip (non-contact mode).

Extremely sensitive controls of the interaction between the AFM tip and the Si surface atoms have resulted in many interesting and diverse manipulations of surface atoms. The experiments demonstrated the extraction of a single atom embedded in the surface lattice. Then the researchers repeated control experiments and revealed that the extracted or an atom from the AFM tip could be deposited back into the defect hole in the surface lattice which was created by the extraction control [OCY$^+$03]. In other experiments of atomic control, a single atom embedded in a surface lattice could be pushed (or pulled) and be rolled over to the top of the surface and then could be dragged laterally by AFM tip [OCAM06]. And in another experiment on the surface with mixed atoms, indium (In) atoms doped on the silicon surface, the atom control experiments with NCAFM showed that

two different type of neighboring atoms could interchange their lattice position [SCAM06]. And another recent experiment succeeded in interchanging two atoms vertically and those atoms were coming as an atom in the surface and one in the AFM tip [SPC$^+$08]. More surprisingly this interchange control was reversible by making another vertical interchange and bringing the original atom into the place. So literally, the experiments in Morita group have shown that any physically imaginable manipulations would be possible. These amazing achievements have been resulted with their state of art NCAFM machines which were home-built by the research group.

4.2 Theoretical studies

There have been two major directions for theoretical explanations of these results. The first avenue of reasoning [TWKS07, Hla05] centers on the consideration of double well potential model within the framework of classical mechanics. When the AFM tip is far away from the lattice, there are two minima of potential energy for the target atom, one close to the tip and another one close to the surface. These potential minima are separated by a large energy barrier that prevents the target atom from reaching the tip. When the AFM tip is within several Angströms (Å) from the surface, the potential barrier between the two minima disappears, affording the capture by the tip; upon tip withdrawal, the potential barrier reappears and the target atom follows the tip. Since the potential well is asymmetric, this line of reasoning leads to the conclusion that there must be a strong preference towards extraction versus deposition of target atoms. Later in this paper we show that it is not necessary for the potential well to disappear completely, and both extraction and deposition may happen even when a finite potential barrier exisits,

as illustrated on Fig. 4.3 and the discussion focusing on the energy balance. We shall note, however, that the double well structure of the potential plays an important role in our considerations, eventually explaining the asymmetry between target atom behavior for deposition and extraction.

Quantum mechanics offers an alternative to the double well mode by allowing the target atom to escape even when the potential barrier is higher than the particle's energy. This is due to the phenomenon of tunneling (*i.e.*, particle crossing the classically forbidden zone) as well as possible changes in the barrier because of the covalent bonding structure. Thus, the second avenue of reasoning appealed to the quantum mechanical explanations [DvP05, Dv07]. Under this paradigm, the Car-Parrinello molecular dynamics (CPMD) model was used to compute the electronic structure for a given configuration of the tip and the lattice. Then, the target atom was moved to find minimal energy state according to the electronic density, and the calculation was repeated again. This quantum mechanical model reproduces some aspects of atomic manipulations along a crystal surface. However, analogously to the classical models described above, these quantum mechanical theories did not consider the time scales of atomic vibration and AFM tip. In other words, these quantum mechanical models assumed the experiment is conducted at absolute zero temperature [DvP05]. However, laboratory evidence at non-zero temperature demonstrates that proper excitation of atomic vibrations has the ability to break chemical bonds [ZFT$^+$06], so the vibrations of individual atoms may alter the results of CMPD dynamics considerably.

4.3 Problem setup

The most interesting to us is the failure of these theories to explain both deposition and extraction of target atom for the same experimental conditions. This is a

natural consequence of considering the atomic manipulation through the prism of force balance only. Indeed, deposition would require a stronger bond between the lattice and the target as compared to tip–target bond. On the other hand, atom extraction would require a stronger tip–target bond as compared to the target–lattice bond. Seen from the point of view of forces only, this creates a paradox precluding the possibility for both deposition and extraction of atoms, which is in apparent contradiction with the experiments [OCY$^+$03].

We show herein that experimental results pertaining to the extraction and deposition can be explained using a purely classical description based on the simple and familiar idea of parametric resonance [Gol01]. Here, by parametric resonance we mean transfer of energy from tip to target atom through a periodic change of a parameter of the system, in our case, the length between these atoms. The idea of parametric resonance-based microscopy has been presented before, see [MMRGHR06]. In our case, we consider parametric resonance as applied to the motion of individual atomic vibrations and not the whole cantilever. In other words, we demonstrate that a coupled dynamics of the AFM tip, target atom and surrounding lattice, is capable of producing excitations which extract or deposit the atoms. The novelty of our approach, compared to the previous literature, lies in the consideration of vibrations for individual atoms. Our explanation proceeds as follows.

A typical time scale of individual atomic vibrations is of the order of 10^{13}Hz [BHT92]. AFM tip itself is an assembly of atomic oscillators – silicon (Si) atoms in experiments – of approximately the same frequency. The dynamics of AFM cantilever oscillation is much slower than the atomic vibrations: the frequency of oscillations of the AFM tip lies in the range of 10^5 Hz. Thus, during one AFM

tip oscillation, each individual atom performs $\sim 10^8$ vibrations. When the AFM tip approaches to the target to about 2 Å, the collective dynamics between the tip and the target ensues due to the arising inter-atomic force between the tip and the target. When the tip stays in near-contact with a target atom on the surface, vibration of the atom in the tip works as a periodic forcing on the target atom and thus amplifies the vibration of target atom. This interaction is a purely classical mechanical effect of parametric resonance. This resonance provides enough energy for a target atom to cross the potential barrier and escape to either the lattice (deposition) or the tip (extraction), without any necessity to either wait for the potential barrier to vanish, or use quantum mechanical tunneling. Also, this scenario allows to explain atomic extraction and deposition using the same physical mechanism.

4.4 Simulations

We conducted simulations on atomic model with pre-defined inter-atomic potential energy to confirm the above scenario on the atomic motion in manipulation control. our simulation model is a simplified 3D model for the dynamics of a single atom under the periodic approach of AFM tip. The set-up for our simulations is illustrated in Fig. 4.1.

The AFM tip which denoted in blue on Fig. 4.1, is represented by five Si atoms in a pyramid configuration with four atoms forming the base, shown in blue. In reality, the Si tip of the AFM will be covered by an oxidized layer [CLK05]. In experiments [MON$^+$03], special care has been taken to remove the oxidization layer from the AFM tip by a stream of inert gas and performing experiments in ultra-high vacuum. Unfortunately, the exact degree of de-oxidization achieved in

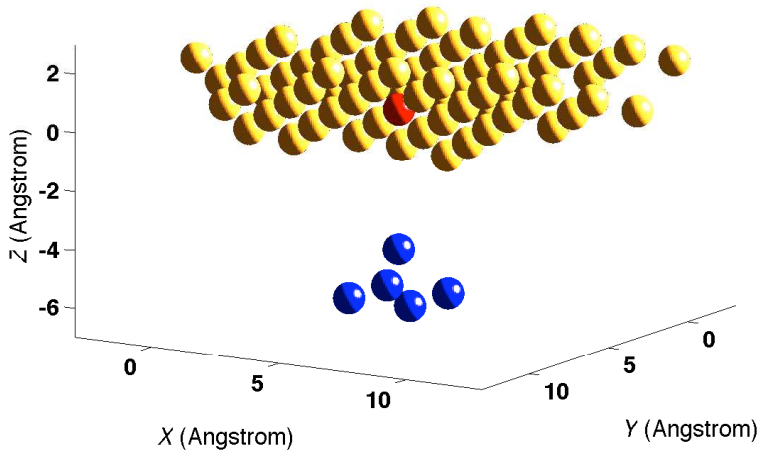

Figure 4.1: Initial arrangement of the lattice atoms (yellow), target atom (red) and AFM tip atoms (blue) for simulations. The tip atoms are considered as fast 5×10^{12} Hz oscillators with fixed amplitude. To model the oscillations of the AFM tip itself, we also prescribe the motion of the tip atoms, bringing them closer to surface and taking them away from the surface with much slower frequency $\sim 10^{10}$ Hz. The dynamics of all 72 target and lattice atoms is then computed according to the rules of Newtonian mechanics, taking into account all the inter-atomic forces.

experiments is not known. In our theory (see below), oxidization will change the atom geometry, oscillation frequency as well as Lennard-Jones interactions. All these factors should impede the manipulation process. The lattice is modeled by 71 atoms in a proper crystal formation (not counting the atomic vibrations), shown in yellow. The target atom, which is identical to lattice atoms, is initially positioned in the place of one of the lattice atoms and is shown in red. Numerical simulation proceeds by computing the dynamics of tip and lattice atoms based on a regular Newtonian mechanics: *mass*$\times$*acceleration* = *net force* for each atom. For simplicity, the AFM tip atoms are modeled by oscillators of fixed frequency, 5×10^{12} Hz, and a fixed amplitude, 0.1 Å, at prescribed time-dependent positions. This amplitude corresponds to the temperature of 80K per oscillation mode as in experiments. It is also a typical value of atomic vibration amplitude reported

earlier [FFQ$^+$94]. Of course, since the temperature is only an averaged measure of energy, it is not applicable to the target and tip atoms. The behavior of the target atom is then a result of many-body dynamics due to atomic interactions.

In this study we shall explain experimental results on atom extraction and deposition at low temperature ($\sim$ 80K) [OCY$^+$03]. Our model assumes only the classical inter-atomic pair potential in the Lennard-Jones (LJ) form:

$$V_{LJ} = 4\epsilon \left[\left(\frac{\sigma}{r}\right)^{12} - \left(\frac{\sigma}{r}\right)^{6} \right] . \tag{4.1}$$

which is similar to the inter-atomic potential observed in the experiments [OCY$^+$03, SPA$^+$07]. It is characterized by strong repulsion in the near field and rapidly diminishing attraction in the far field. The simulation parameters for LJ potential are $\sigma = 2$ Å, $\epsilon = 3.47 \times 10^{-19}$J ($\sim$ 2.17 eV), where ϵ is the minimum energy for the pair potential. In the experiments, the target atom is surrounded by the atoms of the crystalline lattice, with the average distance between two lattice atoms being 2 Å, corresponding to a typical value for a real silicon crystal. The pair potentials between lattice atoms and for target and tip interaction are adjusted to conform to the experimentally measured values of interaction and binding energy in the lattice. The binding energy between two atoms is about -2.5 eV and the binding energy of an atom which is embedded in a bulk lattice is about $-4 \sim -5$ eV with a distance of 2 Å between the atoms [BHT92]. Also, in our simulations, all the atoms are assumed to have the mass of a silicon atom, *i.e.*, 4.648×10^{-26} kg.

In general, other potentials may be used in simulations as well. The important feature for our scenario to be valid is: a) similar frequencies of atomic vibrations for all atoms (tip, target and lattice), and b) the relatively short range of the potential so parametric resonance occurs when the AFM tip comes close to

the lattice. A reasonably accurate approximation of covalent bonds by potential could be possible, although it would require use of more algebraically complex and direction-dependent interaction potentials. We believe that as long as the potential used for modeling of covalent bonds is short range and does not alter atomic vibration frequency significantly, it will lead to similar parametric excitation of atoms. In the absence of good analytical formulas approximation covalent bonds as classical potential we shall leave these studies to the future. Our goal here is to demonstrate that even the simplest LJ potential can explain atomic manipulations. The oscillation of a real-life AFM tip is a periodic function with amplitude ~ 10 nm and frequency $10^5 - 10^6$ Hz. In the simulations, we take a tip performing harmonic oscillations with the same amplitude, but increase the frequency to 10^{10} Hz in order to speed up the computations. This is necessary because we need to resolve the individual atomic vibrations that have a typical frequency of 10^{13} Hz. One AFM oscillation in our simulation thus contains about 10^3 atomic vibrations. The Lennard-Jones potential is effectively felt when the tip atom and the target atom are about $2 - 3$ Å apart. During this time, in our simulations, about 300 atomic vibrations happen, as compared to $10^7 - 10^8$ atomic vibrations during contact in experiment. Unfortunately, resolving a realistic number of atomic oscillations for the complex system we consider is out of reach for modern computers. For real systems, the number of atomic vibrations in contact will increase the energy being transferred from the tip to target atom, although not proportionally because of the nonlinear nature of the resonance. Thus, we expect that atomic manipulation in a corresponding experiment will be easier to achieve. On the other hand, even in this reduced setting we are able to demonstrate target atom extraction and deposition.

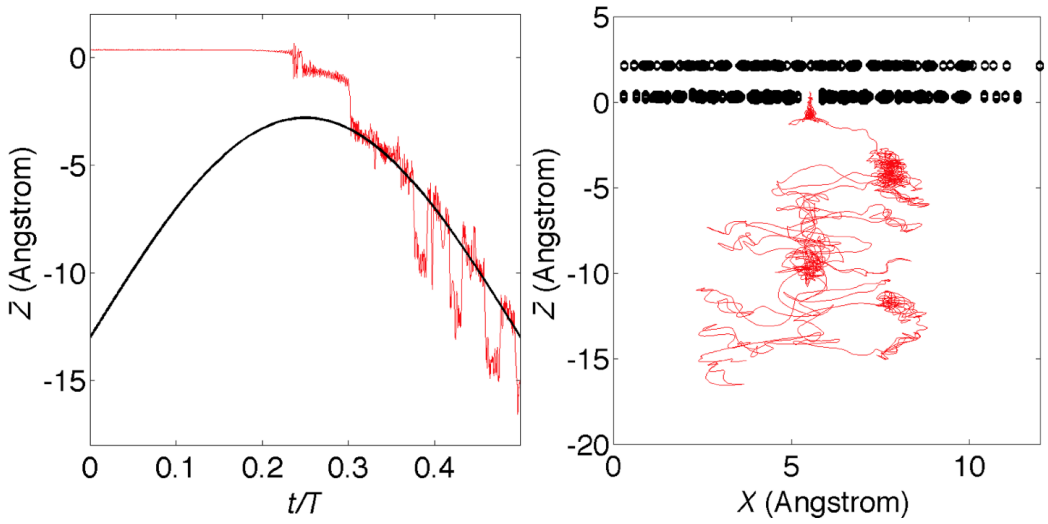

Figure 4.2: Dynamical description of the process of extraction. *Left*: The target atom (thin red line) gets extracted from the lattice under the approach of AFM tip atom, shown in black. Time scale is shown in units of the period T of AFM oscillation. Only the first half of AFM oscillation is shown, as it demonstrates the approach to the lattice. The second half of AFM oscillation plays no role in the dynamics. The target atom follows the tip, escaping the bonds with the lattice. *Right*: The motion of lattice atoms, shown in black, and the target atom, shown in red, as seen from the side. Coordinate X is along the surface, and Z is normal to the surface.

Fig. 4.2, left shows the distance of target atom measured normally to the surface as a function of time. One can see that when the AFM tip (shown as a black line) approaches the target atom, a radical increase of the kinetic energy happens (shown in red). The increased kinetic energy allows the target atom to cross the potential barrier and escape the lattice to join the tip atoms. Side view of target atom extraction is shown in Fig. 4.2, right. Note large meanderings of the target atom (red trajectory) under the extraction process, and relatively small oscillations of lattice atoms, shown in black.

In Fig. 4.3 we illustrate the energy balance of the system. The left part of that Figure shows the double well structure of the potential for different distances of

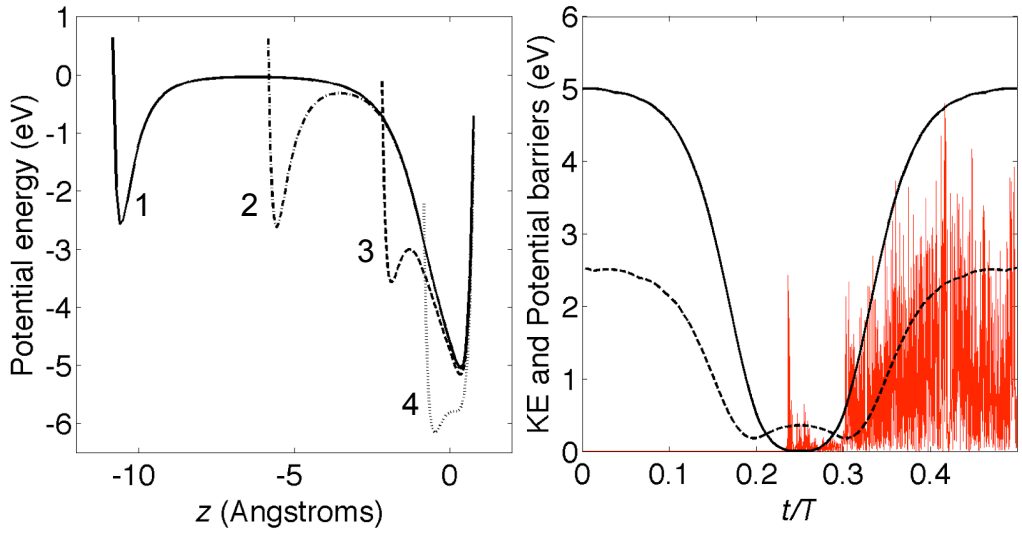

Figure 4.3: Energy balance in the extraction simulation. *Left*: potential energy profile as a function of normal distance Z from the lattice for different separations d of tip apex from the surface. 1 (solid black): $d = 13$ Å; 2 (long dashes): $d = 8$ Å; 3 (short dashes): $d = 4$ Å; 4 (dots): $d = 3$ Å. *Right*: time evolution of potential barriers for the target atom and kinetic energy (KE) of the target atom. Solid black: potential barrier value for the lattice well. Dashed: potential barrier for the tip well. Red is kinetic energy. All energy values are in electron Volts (eV).

AFM tip apex to the lattice surface. Right part of Fig. 4.3 compares the kinetic energy of the target atom and the values of potential barrier of the tip side (dashed) and lattice side (solid black). Initially, the kinetic energy of the target atom is much smaller than the depth of the potential well, but upon the approach of the tip, the kinetic energy quickly increases and at the same time the potential barrier of the double well potential gets smaller. The target atom escapes to the potential well of the tip and is extracted. The drastic increase of the kinetic energy of the target atom after extraction comes from the continued pumping of energy from tip atoms. In reality, dissipation in the system due to imperfect vacuum and formation of covalent bonds will dampen those vibrations. Here, we shall neglect

the dissipation completely as theoretical modeling for atomic dissipation in this setting is not well established.

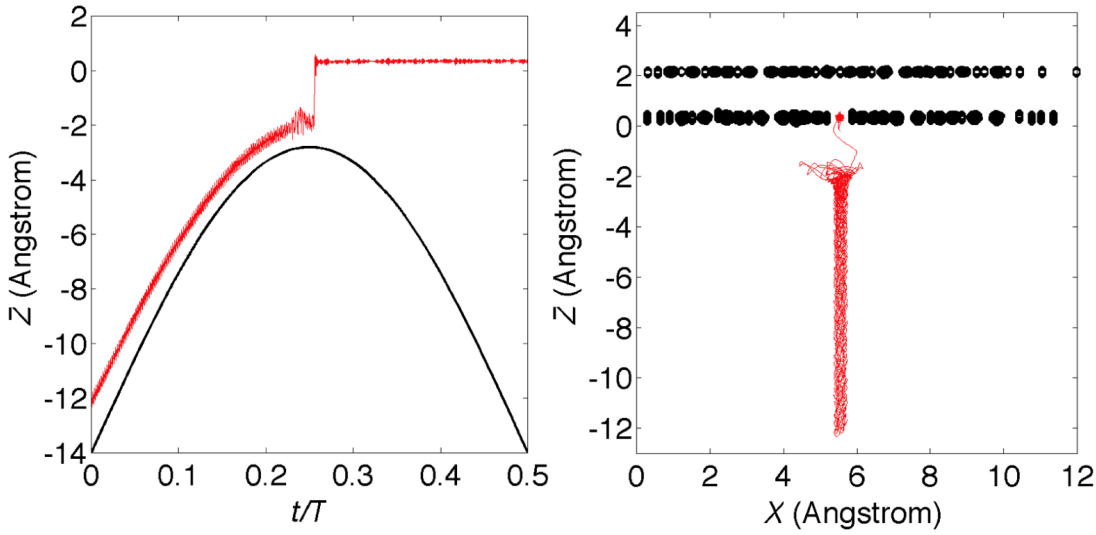

Figure 4.4: Dynamical description of the process of deposition. Left: The target atom (red) follows the AFM tip (blue) until it approaches the lattice, positioned at $Z = 0.2$ Å. Time is scaled by the period of AFM oscillation T. The increase in kinetic energy of the target atom due to the interaction with the lattice atoms allows it to escape the potential well of the tip and bond to the lattice. Right: The motion of lattice atoms, shown in black, and the target atom, shown in red, as seen from the side. Compare to the corresponding dynamics of extraction as shown on Fig. 4.2.

4.5 Discussion

Our models demonstrate the deposition procedure simply by replacing the apex atom of the AFM tip by the target atom. The dynamical process of deposition is illustrated on Fig. 4.4. All the notation is identical to Fig. 4.2 for simplicity of reading. The dynamics of deposition is rather different from that of the extraction due to different values of potential well in the double-well potential as shown on Fig. 4.3, left. The potential well at the tip is much shallower than then potential

well at the surface. Once the atom at the tip acquires sufficient energy to escape from the potential minimum at the tip, that atom will necessarily go directly to the deeper potential minimum at the surface. Thus, the escape from the tip occurs almost instantaneously after the target atom's kinetic energy reaches the value of the potential barrier, as shown on Fig. 4.3, right. Correspondingly, since the total energy of the target atom is small during deposition, the subsequent oscillations of target atom are rather small, as can be seen by comparing the right part of Fig. 4.3 and Fig. 4.2. Our results illuminate the nature of asymmetry between the extraction and deposition as a consequence of a complex interplay between forces of interactions of individual atoms, atomic vibrations and resonance.

In conclusion, we propose a new explanation of extraction and deposition of atoms using AFM. We demonstrate that a simple model of atomic lattice, target atoms and AFM tip, built exclusively on pair potentials and classical mechanics of atoms, can explain both extraction and deposition of atoms. Our explanation is built on the idea of parametric resonance between the vibrating atoms of AFM tip and the target atom. In spite of simplified nature of our models, such as absence of valence bonds, shorter time scales, and rather idealistic view of AFM tip, our results demonstrate the importance of atomic vibrations for the explanation of atomic extraction and deposition. As far as we know, this physical effect has not been considered in previous literature based on either quantum or classical mechanical theories. We thus believe that dynamical effects such as atomic vibrations and resonances are very important for accurate theoretical explanation of atomic manipulations.

Chapter 5

CONCLUSION

This study has been focused on the time-evolution of a rigid body and its applications to nano-scale particles. The time-evolution of objects in nature is complicated. The evolution equations could be obscure when the studied system involves large quantity of atomic elements such as quantum particles or constraint conditions. The tools we have employed in this study are differential equations, symmetries and related mathematical concepts in the effort to understand the evolution of rolling rigid body or atomic system.

On the rigid body motion of Chaplygin's ball, we applied Lie symmetries and a nonholonomic version of Noether symmetries to clarify the origin of conservation laws. These symmetries are applied partially successful in deriving the Jellett and Routh integrals, but still the mechanism for the origin of such first integrals is not yet clearly understood. Further study will be pursued to connect symmetries of dynamical systems under constraints with conservation laws.

The mechanical system of particles with nonholonomic constraint is simulated and analyzed for the application of the concepts in statistical mechanics. The most fundamental concepts in statistical mechanics such as ensemble distribution and temperature, are applied on the nonholonomic system. We observed that the idea of statistical mechanics could be defined and applied on such system. Thus, the

nonholonomic system seems to allow the development of statistical mechanics. In our future study, we will try to apply more complicated and advanced concepts and structures of the thermodynamics on the nonholonomically constrained system.

In the future study, more complicated and advanced concepts and structures of the thermodynamics may be applied on the nonholonomically constrained system. The last chapter of this dissertation discussed the evolution of atomic dynamics during the manipulation process of single atoms. Our analysis utilized the ideas of classical mechanics. Moreover, our proposal brought the manipulation process into a simple and clear picture of particle motions. However, the surface lattice of silicon is an extremely complicated system that contains many electrons between the nuclei, which are considered as simple particles in our study. Hence, further study of considering such quantum particles of electrons in the resonant effect is necessary in order to confirm our mechanism that is proposed for the manipulation process of single atoms.

Bibliography

[BHT92] H. Balamane, T. Halicioglu, and W. A. Tiller, *Comparative study of silicon empirical interatomic potentials*, Physical Review B **46** (1992), 2250–2279.

[Bla] D. N. Blauch, *Kinetic molecular theory.*

[Blo03] A. M. Bloch, *Nonholonomic mechanics and control*, Springer-Verlag, NY, 2003.

[BM02a] A. V. Borisov and I. S. Mamaev, *On the history of the development of the nonholonomic dynamics*, Reg. Chaot. Dyn. **7** (2002), 43.

[BM02b] ———, *Rolling of a rigid body on plane and sphere. hierarchy of dynamics*, Reg. Chaot. Dyn. **7(2)** (2002), 177.

[BMR97] L. Bartels, G. Meyer, and K. H. Rieder, *Basic steps of lateral manipulation of single atoms and diatomic clusters with a scanning tunneling microscope tip*, Phys. Rev. Lett. **79** (1997), no. 4, 697–700.

[BMZ05] A. M. Bloch, J. E. Marsden, and D. V. Zenkov, *Nonholonomic dynamics*, Notices Amer. Math. Soc **52** (2005), 324.

[BPvGH81] H. J. C. Berendsen, J. P. M. Postma, W. F. van Gunsteren, and J. Hermans, *Interaction models for water in relation to protein hydration*, p. 331, Reidel. Dordrecht, Holland, 1981.

[BRMR08] N. M. Bou-Rabee, J. E. Marsden, and L. A. Romero, *Dissipation – induced heteroclinic orbits in tippe tops*, SIAM Review **50** (2008), no. 2, 325–344.

[Cha02] S. A. Chaplygin, *On a ball's rolling on a horizontal plane*, Reg. Chaot. Dyn. **7(2)** (2002), 131.

[CLK05] K.-H. Chung, Y.-H. Lee, and D. E. Kim, *Characteristics of fracture during the approach process and wear mechanism of a silicon afm tip*, Ultramicroscopy **102** (2005), 161–171.

[CMF+09] J. Carrasco, A. Michaelides, M. Forster, S. Haq, R. Raval, and A. Hodgson, *A one-dimensional ice structure built from pentagons*, Nat. Mater. **8** (2009), 427.

[Dv07] P. Dieška and I. Štich, *Simulation of lateral manipulation with dynamic afm : interchange of sn and ge adatoms on ge(111)-c(2 x 8) surface*, Nanotechnology **18** (2007), no. 8, 084016.1–084016.6.

[DvP05] P. Dieška, I. Štich, and R. Pérez, *Nanomanipulation using only mechanical energy*, Phys. Rev. Lett. **95** (2005), no. 12, 126103.1–126103.4.

[ES90] D. M. Eigler and E. K. Schwizer, *Positioning single atoms with a scanning tunneling microscope*, Nature **344** (1990), 524–526.

[FFQ+94] G. E. Franklin, E. Fontes, Y. Qian, M. J. Bedzyk, J. A. Golovchenko, and J. R. Patel, *Thermal vibration amplitudes and structure of as on si(001)*, Physical Review B **50** (1994), 7483–7487.

[GL] L. C. Gomes and R. Lobo, *Statistical mechanics of systems subject to constraints*, Revista Brasileira de Física.

[GN00] C. G. Gray and B. G. Nickel, *Constants of the motion for nonslipping tippe tops and other tops with round pegs*, Am. J. Phys. **68** (2000), 821.

[Gol01] H. Goldstein, *Classical mechanics*, 3rd ed., Addison Wesley, 2001.

[Hla05] S. W. Hla, *Scanning tunneling microscopy single atom/molecule manipulation and its application to nanoscience and technology*, J. Vac. Sci. Technol. B **23(4)** (2005), 1351–1360.

[Koz92] V. V. Kozlov, *The problem of realizing constraints in dynamics*, J. Appl. Maths Mechs **56** (1992), 594.

[KPH09] B. Kim, V. Putkaradze, and T. Hikihara, *Manipulation of single atoms by atomic force microscopy as a resonance effect*, Phys. Rev. Lett. **102** (2009), 215502.

[Kum10] P. Kumar, *Dynamics of 2d monolayer confined water in hydrophobic and charged environments*, 2010.

[Kut99] R. Kutteh, *New approaches for molecular dynamics simulations with nonholonomic constraints*, Computer Physics Communications **119** (1999), 159–168.

[KYX+06] P. Kumar, Z. Yan, L. Xu, M. G. Mazza, S. V. Buldyrev, S. H. Chen, S. Sastry, and H. E. Stanley, *Glass transition in biomolecules and the liquid-liquid critical point of water*, Phys Rev Lett **97** (2006), 177802.

[LL80] L. D. Landau and E. M. Lifshitz, *Statistical physics, part 1*, 3rd ed., Pergamon Press, Oxford, NY, 1980.

[LM95] A. D. Lewis and R. M. Murray, *Variational principles for constrained systems: Theory and experiment*, Int. J. Nonlinear Mech. **30** (1995), 793.

[MKL02] S. Maruyama, T. Kimura, and M. Lu, *Molecular scale aspects of liquid contact on a solid surface*, Thermal Sci. Eng. **10** (2002), no. 6, 23–29.

[MMRGHR06] M. Moreno-Moreno, A. Raman, J. Gomez-Herrero, and R. Reifenberger, *Parametric resonance based scanning probe microscopy*, Applied Physics Letters **88** (2006), 193108.

[MON+03] S. Morita, N. Oyabu, R. Nishi, K. Okamoto, M. Abe, Ó. Custance, I. Yi, and Y. Seino, *Atom selective imaging and mechanical atom manipulation based on noncontact atomic force microscope method*, e-J. Surf. Sci. Nanotech. **1** (2003), 158–170.

[MXSS98] P. B. Miranda, L. Xu, Y. R. Shen, and M. Salmeron, *Icelikewater monolayer adsorbed on mica at room temperature*, Phys. Rev. Lett. **81** (1998), 5876.

[OCAM06] N. Oyabu, Ó. Custance, M. Abe, and S. Morita, *Mechanical atom manipulation and artificial nanostructuring at low temperature*, e-J. Surf. Sci. Nanotech. **4** (2006), 1.

[OCY+03] N. Oyabu, Ó. Custance, I. Yi, Y. Sugawara, and S. Morita, *Mechanical vertical manipulation of selected single atoms by soft nanoindentation using near contact atomic force microscopy*, Phys. Rev. Lett. **90** (2003), no. 17, 176102.1–176102.4.

[Olv93] P. Olver, *Applications of lie groups to differential equations*, 2nd ed., Springer-Verlag, NY, 1993.

[RDG94] G. Reiter, A. L. Demirel, and S. Granick, *From static to kinetic friction in confined liquid films*, Science **263** (1994), 1741.

[SC04] J. A. Stroscio and R. J. Celotta, *Controlling the dynamics of a single atom in lateral atom manipulation*, Science **306** (2004), 242–247.

[SCAM06] Y. Sugimoto, Ó. Custance, M. Abe, and S. Morita, *Site-specific force spectroscopy and atom interchange manipulation at room temperature*, e-J. Surf. Sci. Nanotech. **4** (2006), 376.

[SOZ+06] Y. Shirai, A. J. Osgood, Y. Zhao, Y. Yao, L. Saudan, H. Yang, C. Yu-Hung, L. B. Alemany, T. Sasaki, J. F. Morin, J. M. Guerrero, K. F. Kelly, and J. M. Tour, *Surface-rolling molecules*, J. Am. Chem. Soc. **128** (2006), 4854–4864.

[SPA+07] Y. Sugimoto, P. Pou, M. Abe, P. Jelinek, R. Pérez, S. Morita, and Ó. Custance, *Chemical identification of individual surface atoms by atomic force microscopy*, Nature **446** (2007), 64–67.

[SPC+08] Y. Sugimoto, P. Pou, Ó. Custance, P. Jelinek, M. Abe, R. Pérez, and S. Morita, *Complex patterning by vertical interchange atom manipulation using atomic force microscopy*, Science **322** (2008), 413.

[Tar05] V. E. Tarasov, *Thermodynamics of few-particle systems*, Int. J. Mod. Phys. B **19** (2005), no. 5, 879.

[TSZ04] Q. Tang, S. Q. Shi, and L. Zhou, *Nanofabrication with atomic force microscopy*, Journal of Nanoscience and Nanotechnology **4** (2004), 948–963.

[Tuc] M. Tuckerman, *Statistical mechanics*.

[TWKS07] T. Trevethan, M. Watkins, L. N. Kantorovich, and A. L. Shluger, *Controlled manipulation of atoms in insulating surfaces with the virtual atomic force microscope*, Phys. Rev. Lett. **98** (2007), no. 2, 028101.

[Ulm96] A. Ulman, *Formation and structure of self-assembled monolayers*, Chem. Rev. **96** (1996), 1533–1554.

[ZFT+06] L. Zhiheng, L. C. Feldman, N. H. Tolk, Z. Zhenyu, and P. I. Cohen, *Desorption of h from si(111) by resonant excitation of the si-h vibrational stretch mode*, Science **312,** (2006), no. 5776, 1024–1026.

[ZM03] R. Zangi and A. E. Mark, *Monolayer ice*, Phys. Rev. Lett. **91** (2003), 025502.